JOURNAL OF GEOPHYSICAL RESEARCH, VOL. 113, C03S90, doi:10.1029/2007JC004269, 2008

Trends in Antarctic annual sea ice retreat and advance and their relation to El Niño–Southern Oscillation and Southern Annular Mode variability

S. E. Stammerjohn,[1,2] D. G. Martinson,[1,2] R. C. Smith,[3,4] X. Yuan,[1] and D. Rind[5]

Received 7 April 2007; revised 14 November 2007; accepted 11 February 2008; published 14 March 2008.

[1] Previous studies have shown strong contrasting trends in annual sea ice duration and in monthly sea ice concentration in two regions of the Southern Ocean: decreases in the western Antarctic Peninsula/southern Bellingshausen Sea (wAP/sBS) region and increases in the western Ross Sea (wRS) region. To better understand the evolution of these regional sea ice trends, we utilize the full temporal (quasi-daily) resolution of satellite-derived sea ice data to track spatially the annual ice edge advance and retreat from 1979 to 2004. These newly analyzed data reveal that sea ice is retreating 31 ± 10 days earlier and advancing 54 ± 9 days later in the wAP/sBS region (i.e., total change over 1979–2004), whereas in the wRS region, sea ice is retreating 29 ± 6 days later and advancing 31 ± 6 days earlier. Changes in the wAP/sBS and wRS regions, particularly as observed during sea ice advance, occurred in association with decadal changes in the mean state of the Southern Annular Mode (SAM; negative in the 1980s and positive in the 1990s) and the high-latitude response to El Niño–Southern Oscillation (ENSO). In general, the high-latitude ice-atmosphere response to ENSO was strongest when -SAM was coincident with El Niño and when +SAM was coincident with La Niña, particularly in the wAP/sBS region. In total, there were 7 of 11 -SAMs between 1980 and 1990 and the 7 of 10 +SAMs between 1991 and 2000 that were associated with consistent decadal sea ice changes in the wAP/sBS and wRS regions, respectively. Elsewhere, ENSO/SAM-related sea ice changes were not as consistent over time (e.g., western Weddell, Amundsen, and eastern Ross Sea region), or variability in general was high (e.g., central/eastern Weddell and along East Antarctica).

Citation: Stammerjohn, S. E., D. G. Martinson, R. C. Smith, X. Yuan, and D. Rind (2008), Trends in Antarctic annual sea ice retreat and advance and their relation to El Niño–Southern Oscillation and Southern Annular Mode variability, *J. Geophys. Res.*, *113*, C03S90, doi:10.1029/2007JC004269.

1. Introduction

[2] It is now well established that significant climatic changes are occurring in the Antarctic Peninsula (AP) region, including the adjacent northwestern Weddell and southern Bellingshausen Seas [*Domack et al.*, 2003]. Surface air temperature records from the western AP reveal an annually averaged warming of 2.9°C over 1951–2005 (http://www.antarctica.uk/met/gjma/temps.html). The strongest warming is in winter: 5.8°C over 1950–2005, a warming rate that exceeds any other observed globally [*Vaughan et al.*, 2003], with relatively mild warming of 1.2°C in summer. AP ice shelves and marine glaciers are retreating at rapid rates [*Scambos et al.*, 2003; *Cook et al.*, 2005]. Concurrently, sea ice variability observed over the last two decades of satellite observations show decreases in concentration and duration in the western Antarctic Peninsula/southern Bellingshausen Sea (wAP/sBS) region [*Jacobs and Comiso*, 1997; *Smith and Stammerjohn*, 2001; *Parkinson*, 2002; *Liu et al.*, 2004]. In contrast sea ice concentration and duration are increasing in the western Ross Sea (wRS), while elsewhere in the Southern Ocean sea ice trends are generally weak but mostly positive [*Stammerjohn and Smith*, 1997; *Watkins and Simmonds*, 2000; *Yuan and Martinson*, 2000; *Zwally et al.*, 2002; *Parkinson*, 2004]. The existence of strong opposing regional trends at high southern latitudes where in general the

[1]Lamont Doherty Earth Observatory, Columbia University, Palisades, New York, USA.
[2]Department of Earth and Environmental Sciences, Columbia University, New York, New York, USA.
[3]Institute for Computational Earth System Science, University of California, Santa Barbara, California, USA.
[4]Department of Geography, University of California, Santa Barbara, California, USA.
[5]NASA Goddard Institute for Space Studies, New York, New York, USA.

0148-0227/08/2007JC004269$09.00

climate and atmospheric circulation are more zonally characterized than anywhere else on earth, poses the question as to whether these regional trends are climatically linked, and if so, when and how.

[3] Previous studies have shown that though yearly sea ice duration and monthly sea ice concentration are strongly decreasing in the wAP region, yearly maximum sea ice extent (most equatorward position of the ice edge) is not [*Stammerjohn and Smith*, 1997; *Smith and Stammerjohn*, 2001]. Instead sea ice on average is reaching its most equatorward position but not remaining there as long. Variability and trends in winter sea ice extent mostly reflect variability in the outer pack ice, the area that is most sensitive to wind-forcing, particularly in the wAP region [*Stammerjohn et al.*, 2003; *Harangozo*, 2006]. In winter the ice edge is far removed from the greater expanses of the inner pack ice, yet trends in yearly sea ice duration [*Parkinson*, 2002] and monthly sea ice concentration [*Liu et al.*, 2004] were observed as extending from, and strongest in, the inner pack ice regions. These observations suggest that trends in sea ice duration are resulting from trends in the timing of the autumn-winter advance and/or the spring-summer retreat, and this was the initial impetus for the current study.

[4] Concurrently, in the wAP region there was a strong decrease in monthly sea ice anomaly persistence between the 1980s and 1990s [*Smith et al.*, 1998; *Stammerjohn et al.*, 2003], a decrease from 12–13 months in the 1980s to 2 months in the 1990s (based on autocorrelation analysis) [*Stammerjohn et al.*, 2008]. This somewhat abrupt shift in anomaly persistence between the 1980s and 1990s possibly reflects a considerable increase in ice-atmosphere interactions during the autumn advance and spring retreat. Concurrently, other studies have observed increases in wind speed, cloudiness [*van den Broeke*, 2000] and precipitation [*Turner et al.*, 2005], indicators of increased storminess in the wAP region. Combined, these previous observations suggest that sea ice trends in the wAP region are mostly reflecting changes in ice-atmosphere interactions occurring over spring-autumn during sea ice retreat and subsequent advance.

[5] Seasonal atmospheric circulation variability in the Southern Hemisphere is characterized by the semiannual oscillation (SAO), a twice-yearly intensification and poleward location (60°S–70°S) of the circumpolar atmospheric low-pressure trough during spring and autumn [e.g., *van Loon*, 1967]. Ice-atmosphere interactions associated with the climatological behavior of the SAO largely define the seasonal cycle of sea ice advance and retreat [*Enomoto and Ohmura*, 1990; *Watkins and Simmonds*, 1999; *van den Broeke*, 2000; *Stammerjohn et al.*, 2003]. But, the SAO, and thus sea ice advance and retreat, can be modulated by various climate modes of atmospheric circulation variability. The modes that dominate atmospheric variability in the Southern Hemisphere are the Southern Annular Mode (SAM) [e.g., *Gong and Wang*, 1999; *Thompson and Wallace*, 2000] (also known as the Antarctic Oscillation) and the two Pacific–South American modes associated with the high-latitude response to the El Niño–Southern Oscillation (ENSO) [*Mo and Ghil*, 1987].

[6] The high-latitude response to ENSO and SAM variability is particularly relevant to the examination of any changes in the autumn-winter sea ice advance and spring-summer sea ice retreat, since, over the period studied here (1979–2004), a strong positive trend in SAM has occurred over austral summer-autumn [*Marshall*, 2003; *Marshall et al.*, 2006], while changes in the high-latitude atmospheric response to ENSO have been detected over spring-summer [*Fogt and Bromwich*, 2006]. More specifically, *Fogt and Bromwich* [2006] showed that the high-latitude atmospheric response to ENSO intensified in the 1990s in association with an increase in the covariability between ENSO and SAM (El Niño cooccurring with negative SAM, La Niña with positive SAM), particularly during austral spring (SON), while during austral summer (DJF) ENSO-related SLP anomalies strengthened poleward and eastward toward the Antarctic Peninsula.

[7] In general, SAM variability is characterized by zonally symmetric atmospheric pressure anomalies of opposite sign between Antarctica and midlatitudes [*Thompson and Wallace*, 2000]. Figure 1a shows the regression of sea level pressure onto a SAM index defined by the first principal component of SLP anomalies. Positive atmospheric pressure anomalies at midlatitudes together with negative anomalies at high latitudes indicate a positive SAM (+SAM) and vice versa for a negative SAM (-SAM). Several studies have explored potential connections between Southern Ocean sea ice and SAM [*Hall and Visbeck*, 2002; *Kwok and Comiso*, 2002b; *Lefebvre et al.*, 2004; *Liu et al.*, 2004; *Lefebvre and Goosse*, 2005]. For example, *Lefebvre et al.* [2004] suggest that the regional sea ice response to SAM is associated with the nonannular spatial component of SAM variability, i.e., the significant pressure anomaly in the Amundsen Sea, which is negative during +SAM, and positive during -SAM. This feature creates a meridional component to the otherwise zonally symmetric surface wind stress field such that during +SAM warm northerly winds are found in the western Weddell and Antarctic Peninsula region, while cold southerly winds are found in the Amundsen-Ross Seas (schematically shown in Figure 1a). The northerly winds in turn contribute to negative sea ice anomalies in the western Weddell and Antarctic Peninsula region, and vice versa for southerly winds in the Amundsen-Ross Seas. Further, *Kwok and Comiso* [2002b] show a dipole in surface temperature in response to SAM (similar to the dipole just described for sea ice), and *Lefebvre and Goosse* [2005] show with a global sea ice-ocean model that both thermal and mechanical effects induced by SAM are contributing to the dipole signature in sea ice.

[8] A somewhat similar sea ice variability pattern occurs in response to ENSO variability, where in the western hemisphere of the Southern Ocean (e.g., Ross, Amundsen, Bellingshausen and Weddell Seas) strong covariability between sea ice and ENSO has been shown to prevail [*Gloersen*, 1995; *Harangozo*, 2000; *Kwok and Comiso*, 2002a; *Liu et al.*, 2002, 2004; *Turner*, 2004; *Yuan*, 2004a]. *Yuan* [2004a] provides a thorough conceptualization of potential mechanisms proposed for the high-latitude ENSO teleconnection and sea ice response (her Figure 5b is reproduced in our Figure 1b for a La Niña scenario). One of the primary features of this teleconnection is the weakening of the subtropical jet and a strengthening of the polar front jet in the South Pacific during La Niña events [*Rind et al.*,

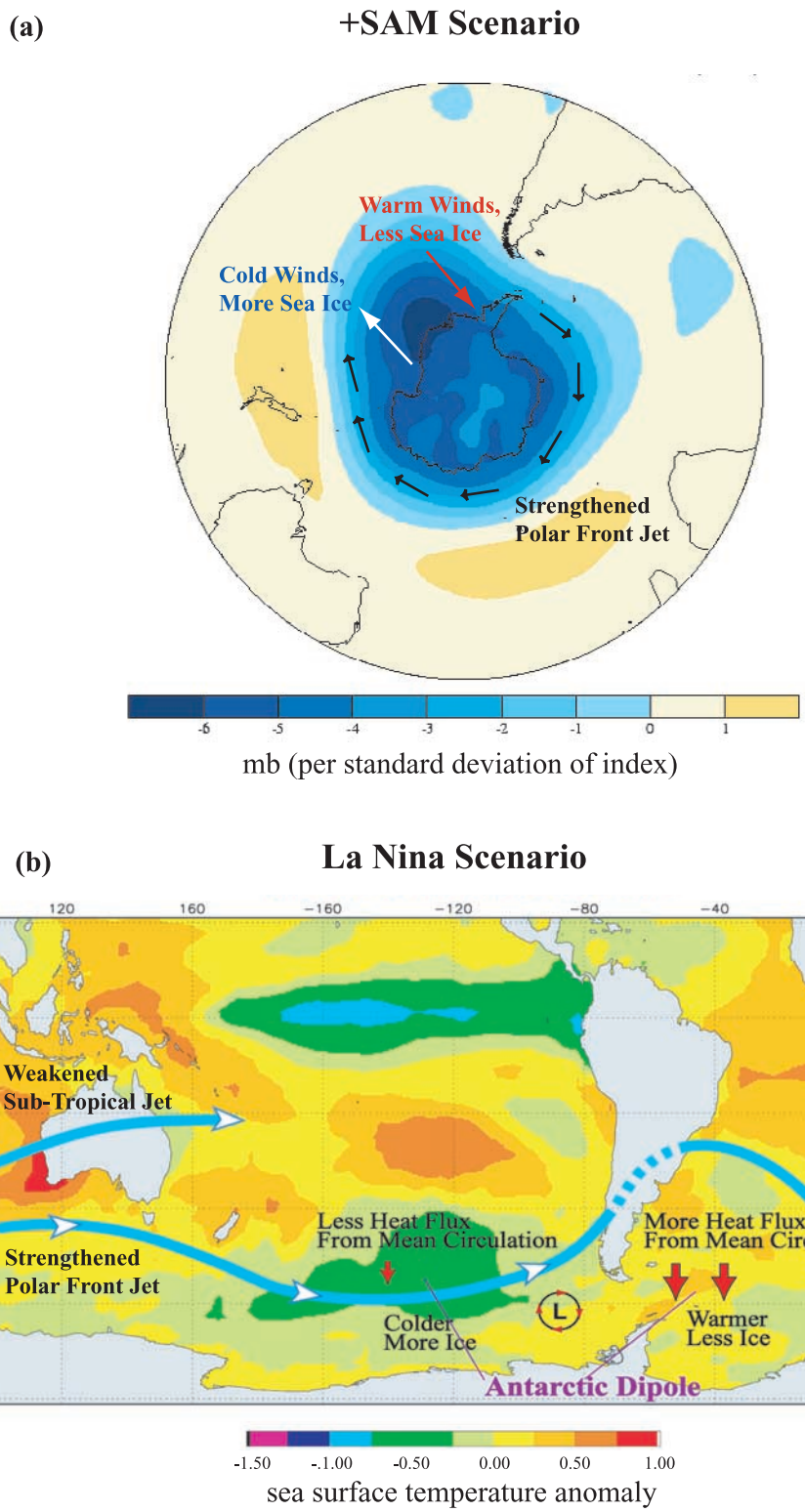

Figure 1. Schematic depiction of the high-latitude ice-atmosphere response to (a) +SAM and (b) La Niña. The base image in Figure 1a is from T. Mitchell (http://www.jisao.washington. edu/sam) and shows the regression of SLP anomalies onto a SAM-derived index (see text and http://transcom.colostate.edu for details). The arrows schematically depict wind anomalies during a +SAM scenario. The image in Figure 1b is adapted from *Yuan* [2004a] (her Figure 5b), with the base map showing a La Niña composite of sea surface temperature anomalies.

2001; *Lachlan-Cope and Connolley*, 2006] (Figure 1b). The strengthening of the polar front jet leads to more storms, warmer conditions and less sea ice in the southern Bellingshausen and western Weddell Seas but colder conditions and more sea ice in the Amundsen and Ross Seas (in association with the spin-up of the quasi-stationary low-pressure cell in the Amundsen Sea). The opposite scenario applies to El Niño events [see *Yuan*, 2004, Figure 5a]. This sea ice anomaly pattern between the Bellingshausen-Weddell Seas and Amundsen-Ross Seas during ENSO events is referred to as the Antarctic Dipole (ADP) [*Yuan and Martinson*, 2001].

[9] The ADP pattern of sea ice variability describes the oscillating high-latitude response to ENSO variability, however as noted above, trends in sea ice duration have been detected in the wAP/sBS region, which lies within the ADP region, as well as in the wRS region, which is peripheral to the ADP region. Also, the ADP pattern of sea ice variability is strongest in the outer pack ice regions, whereas once again, the high-trending regions lie largely within the inner pack ice regions. Nonetheless, this juxtaposition of the high-trending regions versus the ADP region of variability poses the question of how the mechanisms described for the high-latitude response to ENSO variability (as summarized above and depicted in Figure 1b) may, or may not, pertain to the mechanisms underlying the regional trends. We will address this question once we characterize the changes in sea ice advance and retreat.

[10] Finally, there also have been some recent studies that have examined the combined impacts of ENSO and SAM on the high-latitude response of both the atmospheric circulation [*Silvestri and Vera*, 2003; *Carvalho et al.*, 2005; *Fogt and Bromwich*, 2006; *L'Heureux and Thompson*, 2006] and sea ice [*Kwok and Comiso*, 2002b; *Liu et al.*, 2004]. As suggested by *Simmonds and King* [2004] the potential for the high-latitude ENSO response to be modulated by SAM (or vice versa) seems to be greatest in the eastern Pacific sector of the Southern Ocean given the sensitivity of this area to both climate modes. Indeed, the *Liu et al.* [2004] study showed that the sea ice response to ENSO and SAM variability produced regional sea ice concentration anomalies similar to those observed in the wAP/sBS and wRS regions, but the covariability between monthly sea ice concentration versus ENSO and SAM explained only a fractional amount of the overall trends. They concluded that other large-scale processes and/or local feedbacks must be contributing to the trends. At the end of section 5 we will revisit this question of the possible combined influence of ENSO and SAM variability on regional sea ice trends, but from the perspective of when sea ice is retreating (spring-summer) and subsequently advancing (autumn-winter), i.e., the seasons most actively responding to ENSO and SAM variability.

[11] The data and methods used to extract the spatial and temporal variability of sea ice advance and retreat are described next (section 2), followed by an examination of the variability and trends (section 3). Time series from the high-trending regions (wAP/sBS and wRS) are analyzed in detail with respect to regional changes in sea level pressure and ENSO and SAM variability (section 4), followed by a comparison of the spatial changes in the 1980s versus 1990s (section 5). A discussion (section 6) and summary (section 7) conclude the paper.

2. Data and Methods

[12] Satellite measurements of sea ice concentration are from NASA's Scanning Multichannel Microwave Radiometer (SMMR) and the Defense Meteorological Satellite Program's (DMSP) Special Sensor Microwave/Imager (SSM/I). This study uses the GSFC Bootstrap [*Comiso*, 1995] SMMR-SSM/I (quasi) daily time series that minimizes the differences between the various SMMR and SSM/I sensors [*Comiso et al.*, 1997]. The EOS Distributed Active Archive Center (DAAC) at the National Snow and Ice Data Center (University of Colorado at Boulder, http://nsidc.org) provided the every-other-day SMMR and the daily SSM/I time series (January 1979 to December 2004).

[13] As reported by *Comiso et al.* [1997] there are different biases in the derived sea ice concentrations depending on the algorithm used (e.g., NASA Team versus Bootstrap), but in this study we are not tracking sea ice concentration changes but tracking the ice edge as estimated by the 15% sea ice concentration threshold [*Gloersen et al.*, 1992]. Estimates of sea ice extent have relatively high precision due to the large contrast in emissivity between ice and ocean at the frequencies used in sea ice concentration algorithms [*Comiso et al.*, 1997]. Any differences between the various algorithms in estimating the 15% sea ice concentration threshold are largely due to differences in weather masks and are minimal compared to estimates of sea ice concentration >15% [e.g., *Steffen et al.*, 1992]. Also, *Parkinson* [2002] used NASA Team derived sea ice concentrations to determine the length of the sea ice season, and her findings are consistent with ours, inferring that this approach is robust using either algorithm.

[14] Four sea ice characteristics that fundamentally describe the seasonal cycle of sea ice were extracted from (quasi) daily images of SMMR-SSM/I sea ice concentration: (1) day of advance, (2) day of retreat, (3) ice season duration, and (4) actual ice days. When identifying day of advance and retreat, an annual search window is defined such that it begins and ends during the mean summer sea ice extent minimum in mid-February (i.e., begins year day 46, ends year day 410, or 411 if a leap year). Within this interval, day of advance is identified when sea ice concentration first exceeds 15% (i.e., the approximate ice edge) for at least five days. Subsequently, day of retreat is identified when sea ice concentration remains below 15% until the end of the search period. If sea ice never departed from a particular region (e.g., southern Weddell and Amundsen Sea regions), then day of advance and retreat are set to the lower and upper limits, respectively: year day 46 and 410/411. Ice season duration is simply the time elapsed between day of advance and day of retreat, while actual ice days are the number of days between day of advance and retreat when sea ice concentration remained above 15%. Note that *Parkinson* [1994, 2002, 2004] reported on a variable called length of sea ice season, which corresponds to what we call actual ice days.

[15] Numerically analyzed data of sea level pressure (SLP) from the National Center of Environmental Prediction and National Center for Atmospheric Research Reanal-

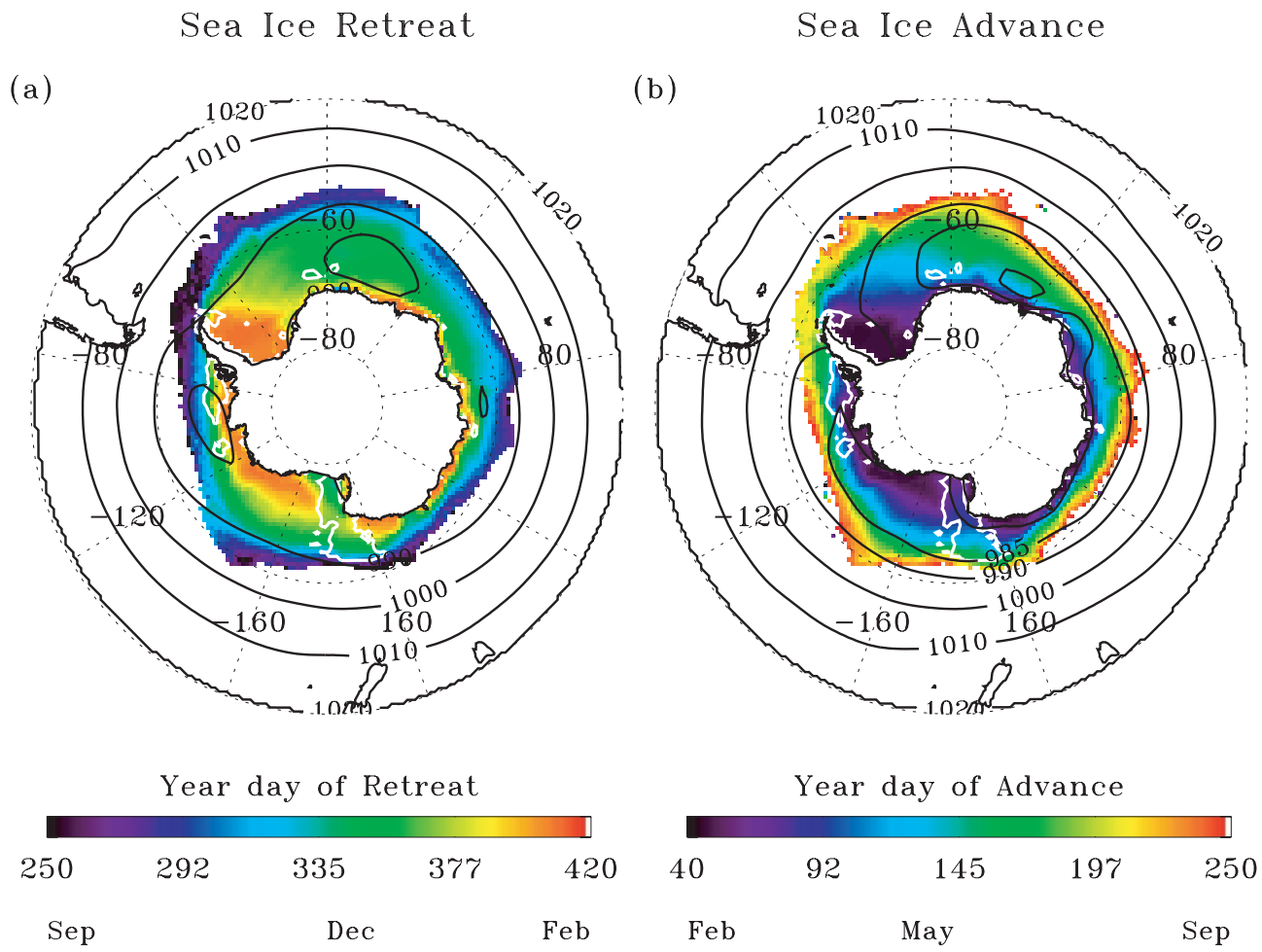

Figure 2. Southern Ocean climatology (1979–2004) for (a) day of retreat and (b) day of advance. White contours correspond to regions showing strong trends (at the 0.01 significance level) in sea ice duration (details provided in Figure 4c). Seasonal climatology (1979–2004) of sea level pressure (SLP, mbar) is shown by the black (labeled) contours for (Figure 2a) December–January–February and (Figure 2b) March–April–May.

ysis (NNR) Project [*Kalnay et al.*, 1996] are used to infer monthly to seasonal changes in regional storm activity. It has been well documented that owing to the sparseness of observational data in the Southern Ocean, there are uncertainties in the quality of the NNR data [e.g., *Drinkwater et al.*, 1999; *Connolley and Harangozo*, 2001; *Bromwich and Fogt*, 2004]. However, with the introduction of satellite data into the numerical data analysis in late 1978 [e.g., *Kanamitsu et al.*, 1997; *Kistler et al.*, 2001], studies have indicated a marked improvement in the NNR data for the Southern Ocean [*Marshall and Harangozo*, 2000; *King*, 2003; *Sturaro*, 2003]. In this study we use NNR data of SLP from 1979 onward.

[16] We also compared variability in the timing of sea ice advance and retreat to ENSO and SAM variability. The ENSO index shown in this study is the Niño 3.4 sea surface temperature index consisting of averaged eastern equatorial Pacific sea surface temperature for 5°N–5°S, 170°W–120°W [*Cane et al.*, 1986] (available at http://iridl.ldeo.columbia.edu/docfind/databrief/cat-index.html). However, we also compared our results to the Southern Oscillation Index (SOI) that consists of the difference between the standardized sea level pressures at Tahiti and Darwin (available at the IRI website given above). In general, we obtain similar results when using either the Niño 3.4 or SOI index (after smoothing the SOI index with a 5-month running mean). The SAM index used here is an observation-based index provided by Gareth Marshall (available at http://www.nerc-bas.ac.uk/icd/gjma/sam.html) [*Marshall*, 2003].

3. Spatial Variability and Trends in Sea Ice Advance and Retreat

3.1. Climatology, Anomalies, and Covariability

[17] On average (1979–2004) sea ice retreat began around September at the most outer edges of the winter pack ice and proceeded southward (poleward) over the next 4–5 months (Figure 2). Most of the retreat of the inner pack ice region occurred over austral summer (DJF), and the climatological SLP pattern showed lower pressures centered roughly on 90°W in the Bellingshausen Sea. Subsequently, the advance began in the most southerly coastal areas in

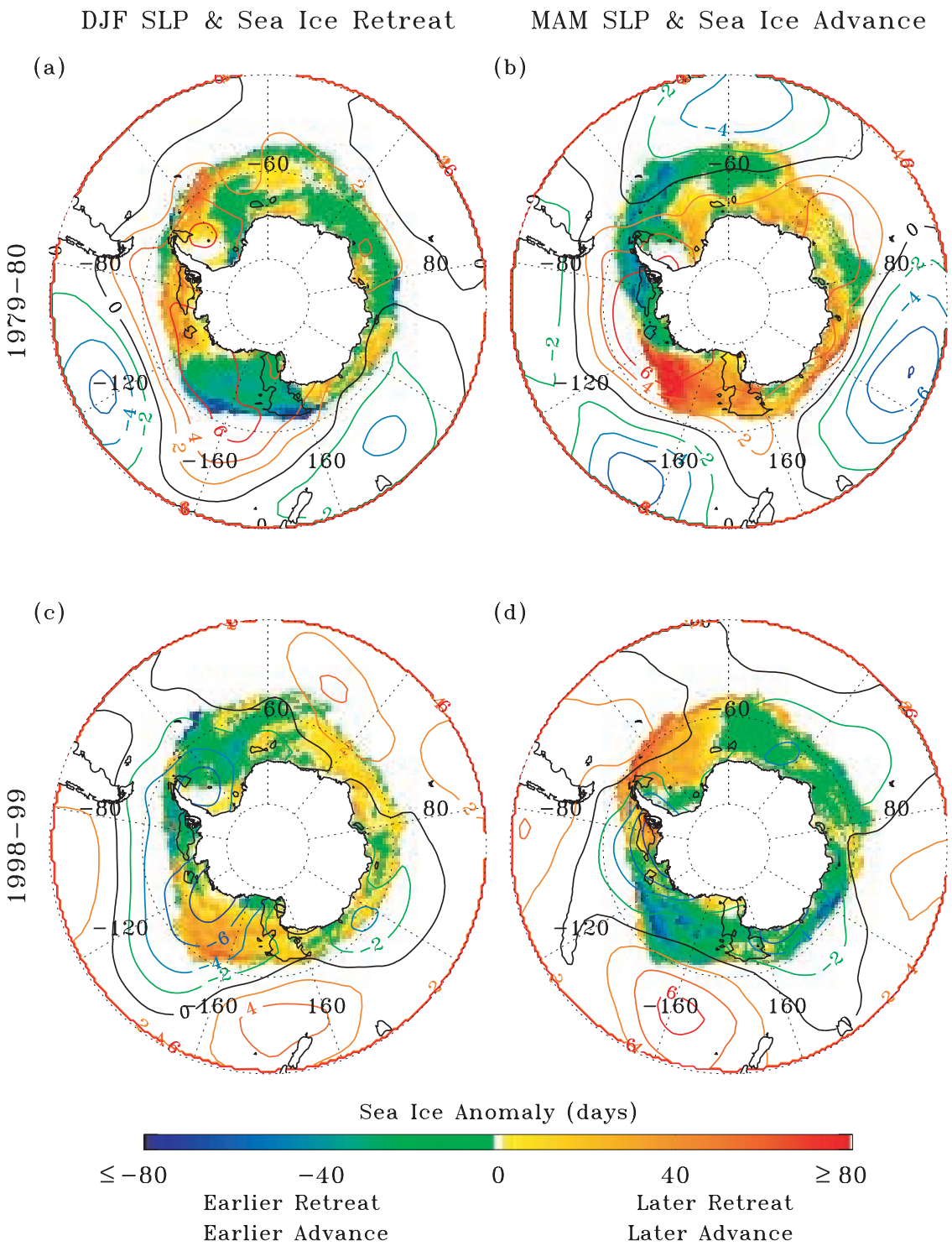

Figure 3. Southern Ocean yearly sea ice retreat and advance anomalies for (a, b) 1979–1980 and (c, d) 1998–1999. Black contours correspond to regions showing strong trends (at the 0.01 significance level) in sea ice duration (details provided in Figure 4c); colored contours are SLP anomalies.

February and progressed northward (equatorward) for the next 7–8 months. Most of advance of the inner pack ice region occurred over austral autumn (MAM), and the climatological SLP pattern showed lower pressures centered roughly on 140°W in the eastern Ross Sea. Concurrently in austral autumn, SLP decreased in the circumpolar trough region (60°S–70°S) in accordance with the SAO (i.e., the deepening of the trough in spring and autumn).

[18] Generally, sea ice anomalies for either retreat or advance showed large areas of spatial continuity, and for large anomaly years, there was a high degree of interseasonal persistence: where the spring-summer retreat was early, the subsequent autumn-winter advance was often late, and

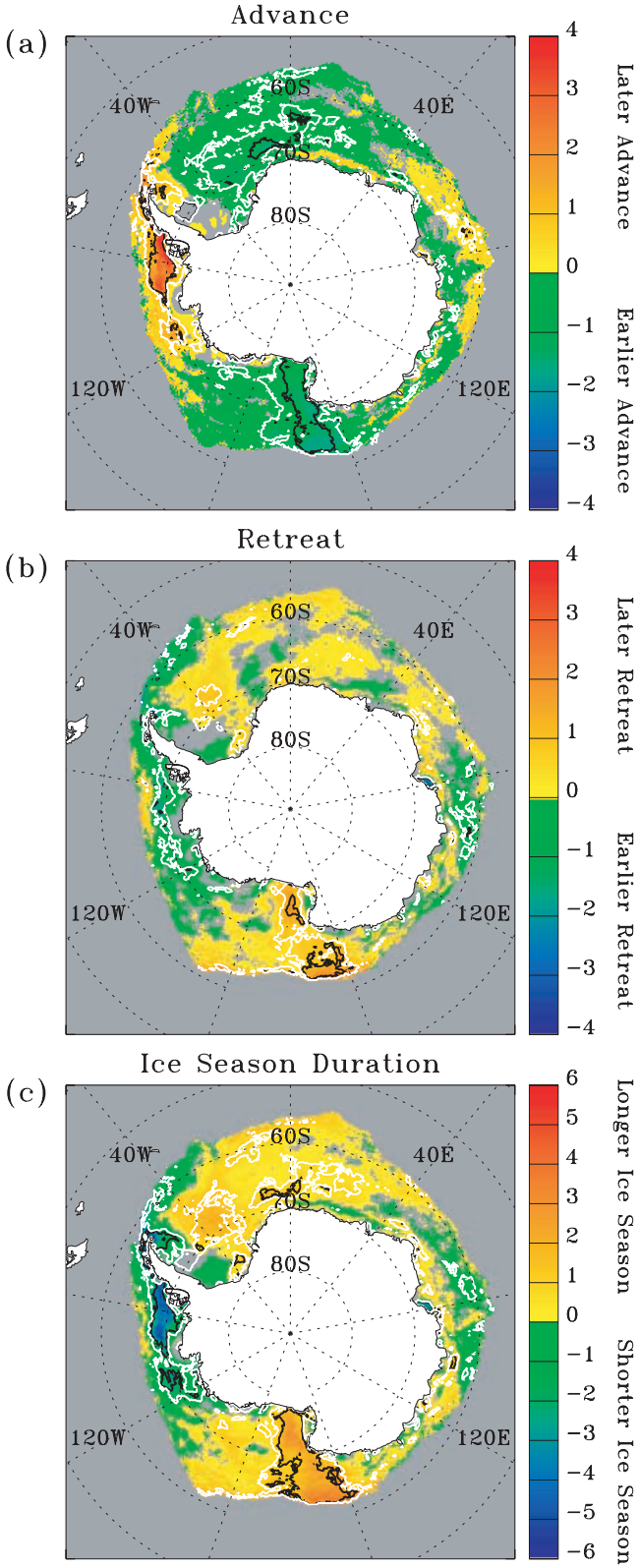

Figure 4. The 1979–2004 trend (days/year) maps of (a) day of advance, (b) day of retreat, and (c) ice season duration. The black/white contours delimit the 0.01/0.10 significance levels. Significance was determined on the basis of effective degrees of freedom following *Santer et al.* [2000]. Within the sea ice zone, gray shading signifies near zero trend.

vice versa for late retreat and early advance (Figure 3). The particular years chosen for Figure 3 exemplify the ice-atmosphere anomaly patterns associated with a strong -SAM (1979–1980) and a strong +SAM/La Niña (1998–1999) and represent two of the largest ice-atmosphere anomaly years in each decade, respectively. (Other very large anomaly years were the +SAM/La Nina in 1988–1989 and the -SAM/El Nino in 1991–1992 that had ice-atmosphere anomaly patterns similar to Figures 3c and 3d and Figures 3a and 3b, respectively). Further, Figure 3 shows the magnitude of regional sea ice changes that, as will be shown shortly, are contributing to strong sea ice trends in the wAP/sBS and wRS regions (i.e., the black contours in the wAP/sBS and wRS regions).

[19] For the 1998–1999 +SAM/La Niña (Figures 3c and 3d) the negative SLP anomaly at high latitudes in the South Pacific resemble those depicted schematically in Figure 1, and the ice-atmosphere response is interpreted as follows. The low SLP anomaly centered on 130°W in DJF (and on 90°W in MAM) was associated with anomalously warm northerly winds along the eastern flank, cold southerly winds along the western flank of the SLP anomaly. In the wAP region for example warm northerly winds assisted an earlier spring sea ice retreat and a later autumn sea ice advance (i.e., assisted both thermally and via wind-driven ice drift), while in the Ross Sea region cold southerly winds assisted a later spring sea ice retreat and an earlier autumn sea ice advance. In contrast, the positive SLP anomaly centered on 120°W in MAM 1980 (Figure 3b) was associated with cold southerly winds over the wAP region, which assisted an early sea ice advance, while warm northerly winds over the Ross Sea assisted a late sea ice advance. As will be shown in section 6.2, the NNR wind data were consistent with the above interpretation.

[20] Although ice season duration by definition is determined by the timing in sea ice advance and retreat, there is the question whether variability in advance or retreat more strongly influences ice season duration and whether there is covariability between sea ice advance and retreat. Correlations between the 26-year time series of ice season duration versus sea ice advance and retreat show that sea ice advance in most regions of the Southern Ocean was more highly correlated to ice season duration than sea ice retreat. In contrast, correlations between sea ice advance and retreat were much weaker, though became stronger when sea ice advance was lagged one year such that variability in sea ice retreat was compared to variability in the subsequent sea ice advance (i.e., variability over spring-autumn versus over autumn-spring). As illustrated in Figure 3, during large anomaly years the spatial extent of anomaly persistence over spring-autumn was particularly strong and observed throughout most of the Southern Ocean.

3.2. Trends

[21] Two regions in particular showed strong and statistically robust trends (as identified by the 0.01 significance level contoured in black) in sea ice advance, retreat and consequently ice season duration: the wAP/sBS and wRS regions (Figure 4). As noted in section 1, *Parkinson* [2004] showed similar results as Figure 4c for trends in length of ice season over 1979–2002, as did *Liu et al.* [2004] for trends in monthly sea ice concentration. In the wAP/sBS

Table 1. Trends (1979–2004) in Advance, Retreat, and Ice Season Duration for the wAP/sBS and wRS Regions, Reported as Total Change Over the 26-Year Period[a]

Region	Day of Advance	Day of Retreat	Ice Season Duration
wAP/sBS	+54 ± 9	−31 ± 10	−85 ± 20
wRS	−31 ± 6	+29 ± 6	+60 ± 10

[a]Total change is given in days. The trends for each region were averaged over the area enclosed by the 0.01 significance level (black contour) shown in Figure 4c, with the additional requirement that a nonzero trend value existed in Figure 4a as well: N = 865 pixels for wAP/sBS, and N = 1568 pixels for wRS. The standard error was determined using the effective degrees of freedom present in the regression residuals [*Santer et al.*, 2000].

region a strong trend toward a later autumn advance and a somewhat weaker trend toward an earlier spring retreat resulted in a total decrease of about 2.8 months in ice season duration over 1979–2004 (Table 1). The opposite situation occurred in the wRS region: trends toward an earlier autumn advance and later spring retreat resulted in a total *increase* of about 2 months in ice season duration. As discussed by *Watkins and Simmonds* [2000], the fact that the trend in ice season duration is similar to the trend reported for sea ice concentration (as shown by *Liu et al.* [2004]) indicates that on average higher sea ice concentration occurs when sea ice duration is longer, and vice versa for lower sea ice concentration. Further, these results suggest that trends in sea ice concentration are reflecting trends in the timing of sea ice advance and retreat.

[22] The areas showing the strongest trends in the timing of sea advance and retreat also indicate when large seasonal changes were occurring in the ocean-atmosphere-ice system. For example, the trends in advance in the wAP/sBS and wRS regions occurred when sea ice on average was advancing from mid-February to May in those respective regions (see Figure 2b). However, the ice edge was still advancing after May, especially in the Bellingshausen region, but trends were not detected in the outer pack ice region where sea ice on average was advancing from May to July. We thus infer that the mechanism(s) forcing these trends were strongest during the mid-February to May time period, and similarly from the December to February time period for sea ice retreat, and/or that sea ice advance/retreat was more sensitive to atmospheric forcing during these seasons/locations as discussed further below.

[23] We also note that the trend in actual ice days (not shown) was nearly identical to the trend for ice season duration (Figure 4c), indicating that ice-edge variability occurring after the initial advance and before the final retreat was not large enough to affect the trends imposed by changes in the timing of sea ice advance and retreat. We emphasize again that the highest trending areas were considerably south of the mean equatorward position of maximum winter sea ice extent, i.e., south of the high-variability regions that are sensitive to the quasi-weekly passage of winter storms [*Stammerjohn et al.*, 2003; *Harangozo*, 2004a, 2006]. As discussed by *Harangozo* [2004a, 2006] the synoptic influence on winter ice-edge variability, particularly in the west Antarctic Peninsula region, largely determines the anomalies in maximum winter sea ice extent. However, as we noted in section 1, the ice season duration trend in the west Antarctic Peninsula region appears to be unrelated (at least consistently) to variability in winter maximum sea ice extent. Thus, in contrast to winter sea ice extent variability, trends in ice season duration in the wAP/sBS and wRS regions were (1) mostly south of regions of high winter ice-edge variability, and (2) largely determined by changes occurring during the spring retreat and autumn advance.

[24] To help convey the magnitude of change that occurred in the wAP/sBS region over 1979–2004, in 1979 ice season duration was 365 days (i.e., perennial) for most of the area within the high-trending area of the wAP/sBS region (i.e., within the black contoured wAP/sBS area in Figure 4c). Over 1979–2004 the spatial extent of perennial sea ice decreased, with almost a complete removal of summer sea ice in years 1988–1989 and 1998–1999 [see also *Jacobs and Comiso*, 1997]. In contrast, ice season duration in the wRS region (again, within the black contoured wRS area in Figure 4c) was 208 days (spatially averaged) in 1979. In year 2003 (the highest ice season year observed in the wRS region), sea ice duration increased to 293 days.

4. Ice-Atmosphere Temporal Variability

[25] Given that the trends in annual sea ice duration resulted from changes in the timing of the annual sea ice advance and retreat, we examined those time series in association with atmospheric circulation changes that occurred during 1979–2004, particularly in relation to ENSO and SAM variability. We focused on austral summer (DJF), when sea ice was retreating within the high-trending regions, and the subsequent austral autumn (MAM), when sea ice was advancing in these same regions. The DJF and MAM seasonal averages of sea level pressure (SLP) and Niño 3.4 and SAM indices were computed and compared to the sea ice time series of retreat and advance, respectively (Table 2). Two sea level pressure (SLP) time series were analyzed, one centered on 75°S, 130°W and the other centered on 65°S, 90°W. SLP anomalies in association with ENSO or SAM variability can be found in the vicinity of either of these locations (e.g., Figure 3). Also, *Fogt and Bromwich* [2006] observed an eastward strengthening of ENSO-related atmospheric circulation anomalies in austral summer (DJF) between the 1980s and 1990s, therefore it is of interest to examine the variability of SLP at both 130°W and 90°W, as well as to separately analyze the 1980s and 1990s. Additional incentive for analyzing the 1980s and 1990s separately comes from previous observations showing changes in ENSO-related precipitation in West Antarctica between these two time periods [*Cullather et al.*, 1996; *Bromwich et al.*, 2000; *Genthon and Cosme*, 2003].

[26] For both the DJF and MAM SLP time series, the sign of the correlations between SLP versus Niño 3.4 (positive) and SAM (negative) were as depicted in Figure 1: negative SLP anomalies covarying with negative Niño 3.4 anomalies (or La Niña conditions), and negative SLP anomalies covarying with positive SAM anomalies; vice versa for positive SLP anomalies. However, the correlations between the DJF sea ice retreat and the other indices were in general weak to moderate despite some relatively strong correlations between SLP and Niño 3.4/SAM (Table 2). In other words, there was some ENSO- and SAM-related atmospheric circulation variability detected in the time series but little to

Table 2. Correlations Between Time Series (1979–2004) of Sea Ice Retreat and Advance in the wAP/sBS and wRS Regions Against December–January–February (DJF) and March–April–May (MAM) Seasonal Averages of SLP, Niño 3.4, and SAM[a]

	DJF SLP 130°W	DJF SLP 90°W	DJF Niño 3.4	DJF SAM
wAP/sBS Retreat	**+0.51** (***+0.58***, +0.01)	+0.32 (***+0.57***, −0.13)	+0.18 (+0.39, +0.27)	**−0.53** (−0.33, −0.16)
wRS Retreat	−0.31 (+0.09, −0.49)	−0.16 (+0.09, −0.15)	−0.02 (−0.14, −0.05)	+0.23 (−0.10, +0.14)
DJF SAM	**−0.85** (*−0.63*, **−0.84**)	**−0.53** (***−0.57***, −0.52)	−0.30 (−0.31, ***−0.55***)	
DFJ Niño 3.4	*+0.43* (***+0.60***, *+0.64*)	**+0.49** (+0.40, **+0.87**)		wAP/sBS versus wRS
DJF SLP 90°W	**+0.67** (**+0.85**, *+0.68*)			*−0.41* (+0.54, +0.14)
	MAM SLP 130°W	MAM SLP 90°W	MAM Niño 3.4	MAM SAM
wAP/sBS Advance	**−0.62** (*−0.69, −0.72*)	−0.27 (***−0.59***, −0.53)	−0.32 (*−0.72, −0.66*)	*+0.46* (+0.53, +0.51)
wRS Advance	**+0.70** (**+0.85**, +0.50)	***+0.35*** (*+0.74, +0.63*)	+0.07 (+0.20, +0.50)	**−0.50** (*−0.65*, −0.41)
MAM SAM	**−0.85** (**−0.80**, **−0.88**)	**−0.67** (**−0.88**, −0.51)	−0.14 (−0.15, −0.22)	
MAM Niño 3.4	+0.18 (+0.20, +0.35)	*+0.40* (+0.02, **+0.80**)		wAP/sBS versus wRS
MAM SLP 90°W	**+0.61** (**+0.93**, +0.46)			**−0.68** (−0.52, −0.15)

[a]The two sea level pressure (SLP) time series are from 75°S, 130°W, and 65°S, 90°W. The values in parenthesis correspond to the correlations computed over 1980–1989 and 1990–1999, respectively. Correlations at the 0.01, 0.05, and 0.10 significance level are in bold, italic, and italicized bold, respectively.

none detected in sea ice retreat. In contrast, sea ice advance in both the wAP/sBS and wRS regions showed strong covariability with MAM SLP, which also showed strong correlations with Niño 3.4 and SAM, particularly when the 1980s and 1990s were tested separately.

[27] Consistent with *Fogt and Bromwich* [2006] who observed an eastward strengthening in the 1990s of ENSO-related atmospheric circulation anomalies during DJF, the correlations in Table 2 also indicate similar changes, but for both DJF and MAM time series. For example, correlations between DJF SLP and MAM SLP versus Niño 3.4 were stronger at 130°W than at 90°W in the 1980s, but then became significantly stronger at 90°W in the 1990s. There also appears to be a moderate increase in the negative covariability between ENSO and SAM (El Niño cooccurring with -SAM, and vice versa) in the 1990s, particularly during DJF, less so during MAM. According to *Fogt and Bromwich* [2006], however, the largest increase in ENSO and SAM covariability was in austral spring (SON), with correlations going from −0.01 in the 1980s to +0.71 in the 1990s (tested using the SOI, where -SOI indicates an El Niño and positively covaries with -SAM, and vice versa). They also noted that the 1990s circulation anomalies had a more SAM-like (annular) anomaly pattern and attributed the greater intensification of atmospheric circulation anomalies in the 1990s to the general strengthening of covariability between ENSO and SAM.

[28] Table 2 also indicates that there was higher ENSO-related SLP variability during austral summer (DJF) than during autumn (MAM), while SAM-related SLP variability was high during both DJF and MAM, but particularly during MAM. These seasonal differences in climate covariability are expected since the high-latitude response to ENSO has been strongest in summer [e.g., *Fogt and*

Figure 5. Normalized time series (1979–2004) of March–April–May (MAM) (a) SLP at 65°S, 90°W (dashed line) and Niño 3.4 (solid line), (b) SLP at 75°S, 130°W (dashed line) and SAM (solid line), (c) sea ice advance in the wAP/sBS region (dashed line) and Niño 3.4 (solid line), and (d) sea ice advance in the wRS region (dashed line) and SAM (solid line). Trends lines are shown for (Figure 5a) SLP at 65°S, 90°W (dashed line, -0.08 ± 0.15, $p = 0.30$), (Figure 5b) SLP at 75°S, 130°W (dashed line, -0.16 ± 0.13, $p = 0.11$), (Figure 5c) wAP/sBS advance (dashed line, 2.1 ± 0.35, $p < 0.01$), (Figure 5d) wRS advance (dashed line, -1.2 ± 0.22, $p < 0.01$), and for SAM (solid line, 0.05 ± 0.04, $p = 0.13$) in Figures 5b and 5d. For comparison, the strongest seasonal trends in SLP (at both locations) were in austral summer (DJF): -0.39 ± 0.15, $p = 0.01$ (75°S, 130°W) and -0.23 ± 0.12, $p = 0.04$ (65°S, 90°W), coincident with the strongest seasonal trend in SAM: 0.07 ± 0.03, $p = 0.02$. (Standard error and significance were determined using effective degrees of freedom, which varied from 15 to 23 out of a total of 26 for these time series.)

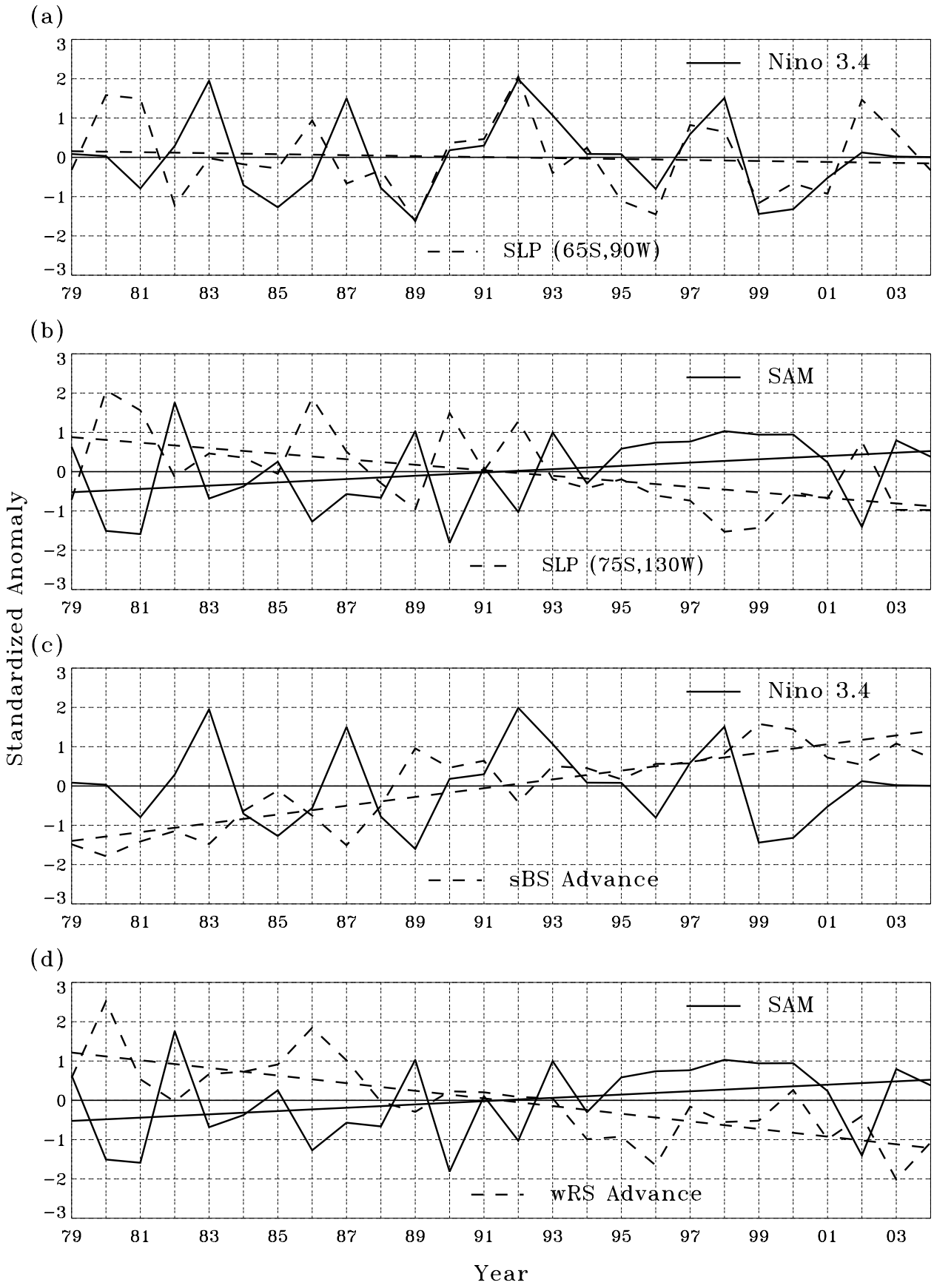
(a)
Nino 3.4
SLP (65S,90W)
(b)
SAM
SLP (75S,130W)
(c)
Nino 3.4
sBS Advance
(d)
SAM
wRS Advance
Standardized Anomaly
Year
3
2
1
0
−1
−2
−3
79
81
83
85
87
89
91
93
95
97
99
01
03

Figure 5

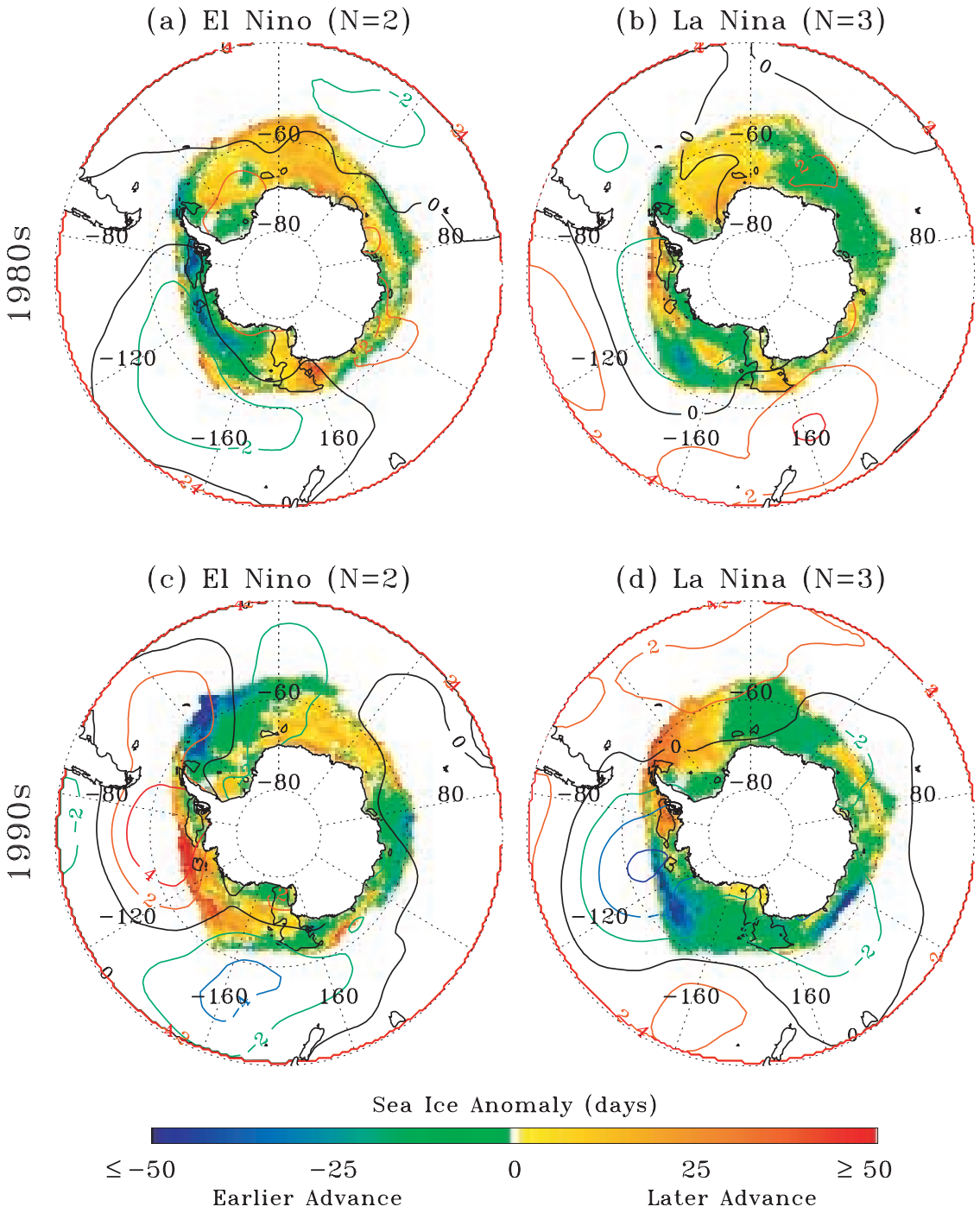

Figure 6. ENSO composites of sea ice advance (color shading) and MAM SLP (color contours) anomalies for the (a) 1980s El Niño (N = 2), (b) 1980s La Niña (N = 3), (c) 1990s El Niño (N = 2), and (d) 1990s La Niña (N = 3). See Table 3 for list of ENSO years used.

Bromwich, 2006], while changes in SAM have been strongest in summer-autumn [e.g., *Marshall*, 2003]. However, the general increase in ENSO-related SLP variability during both SON [*Fogt and Bromwich*, 2006] and MAM in the 1990s is noteworthy and further indicates change in the high latitude response to ENSO.

[29] Of relevance as well are the physical and mechanical differences between the processes of sea ice retreat and sea ice advance. The stronger covariability detected between sea ice advance and the various MAM climate indices may in part be due to the fact that the equatorward expansion of sea ice during advance is unconstrained physically (no continental boundary to the immediate north), thus is able to respond coherently and quickly to changing atmospheric conditions. Also, sea ice advance (more so than sea ice retreat) would be more sensitive to rapid changes in atmospheric conditions given the ability to rapidly vent ocean heat, especially during cold air outbursts. In contrast,

Table 3. Years Used in the ENSO/SAM Composites of Figures 6 and 7, Together With Normalized Values of the March–April–May (MAM) Niño 3.4 and SAM Indices Based on the 1979–2004 Time Series[a]

	MAM Niño 3.4 (std)	MAM SAM (std)	Composite
	1980s		
El Niño/-SAM 1983	+1.95	−0.68	Figure 6a/7a
El Niño/-SAM 1987	+1.50	−0.57	Figure 6a/7a
La Niña 1984	−0.71	(−0.38)	Figure 6b
La Niña 1985	−1.27	(+0.25)	Figure 6b
La Niña 1989	−1.60	(+1.03)	Figure 6b
-SAM 1980	(+0.03)	−1.51	Figure 7b
-SAM 1981	(−0.79)	−1.59	Figure 7b
-SAM 1986	(−0.56)	−1.27	Figure 7b
-SAM 1988	(−0.78)	−0.66	Figure 7b
-SAM 1990	(+0.18)	−1.82	Figure 7b
	1990s		
El Niño 1992	+1.99	(−1.03)	Figure 6c
El Niño 1998	+1.51	(+1.03)	Figure 6c
La Niña/+SAM 1996	−0.80	+0.74	Figure 6d/7c
La Niña/+SAM 1999	−1.44	+0.94	Figure 6d/7c
La Niña/+SAM 2000	−1.32	+0.94	Figure 6d/7c
+SAM 1993	(+1.07)	+1.00	Figure 7d
+SAM 1995	(+0.08)	+0.58	Figure 7d
+SAM 1997	(+0.59)	+0.76	Figure 7d
+SAM 1998	(+1.51)	+1.03	Figure 7d

[a]All years included in the ENSO and/or SAM composites met the requirement that the normalized MAM Niño 3.4 (Figure 6) and/or SAM (Figure 7) index exceeded ±0.5 standard deviation (excepting the values in parentheses). Note that the ±0.5 criteria excluded the otherwise strong austral spring-summer El Niños of 1987–1988 and 1994–1995, but inclusion of those years did not change the spatial patterns shown in Figures 6a and 6c, but did weaken the overall magnitude.

sea ice retreat is constrained physically by the Antarctic continent and by increasing sea ice thickness to the south. These constraints on sea ice retreat would be more pronounced for the inner pack ice regions and perhaps not at all relevant for the outer pack ice regions under divergent conditions [*Stammerjohn et al.*, 2003; *Turner et al.*, 2003; *Harangozo*, 2004a, 2006; *Massom et al.*, 2006, 2008]. Finally and as mentioned previously, variability and trends in sea ice advance (rather than retreat) were more strongly correlated to variability and trends in ice season duration (e.g., Figure 4). In short, the temporal variability in sea ice advance may more readily capture climate signals (e.g., thermal and wind-driven responses due to anomalous storm forcing) given its unconstrained equatorward expansion.

[30] Given this, the rest of our analysis will focus on the temporal and spatial variability of ice-atmosphere interactions during austral autumn (MAM). Several key observations of ice-atmosphere variability during MAM are highlighted in Figure 5 and summarized as follows: (1) both the 1980s and 1990s began with strong positive SLP anomalies (e.g., MAM 1980, 1981, and MAM 1990 and 1992) and ended with strong negative SLP anomalies (e.g., MAM 1989, MAM 1999); (2) in turn, these strong positive SLP anomalies cooccurred with -SAM in 1980, 1981 and 1990 and with -SAM/El Niño in 1992, while the strong negative SLP anomalies in both 1989 and 1999 cooccurred with +SAM/La Niña; (3) the strong positive covariability between SLP (65°S, 90°W) and Niño 3.4 from 1988–2001 is contrasted against little to no covariability prior to 1988 (Table 2: R = +0.02 and +0.80 for MAM SLP 90°W versus Niño 3.4 in the 1980s and 1990s, respectively); (4) the negative covariability between wAP/sBS sea ice advance and Niño 3.4 for all ENSO events is contrasted against the exception during the 1997–1998 El Niño (Table 2: R = −0.72 and −0.66 for wAP/sBS sea ice advance versus MAM Niño 3.4 in the 1980s and 1990s, respectively); (5) the negative covariability between wRS sea ice advance and SAM between 1979 and 1999 is contrasted against the exception during the 1990–1994 period of weak to moderate El Niños (Table 2: R = −0.65 and −0.41 for wRS sea ice advance versus MAM SAM in the 1980s and 1990s, respectively); and finally (6) superimposed on the interannual to decadal variability are trends toward more negative SLP and more positive SAM, together with the opposing trends in sea ice advance between the wAP/sBS and wRS regions.

[31] In general, SAM was mostly negative between 1980 and 1990 (MAM SAM normalized mean was −0.50) but then became mostly positive between 1991 and 2000 (MAM SAM normalized mean was +0.48). It seems likely therefore that, in addition to variability among ENSOs in the tropical Pacific over 1979–2004 [e.g., *Cess et al.*, 2001; *Harangozo*, 2004b; *Trenberth and Smith*, 2006], the change in the mean state of SAM between the 1980s (mostly -SAM) and 1990s (mostly +SAM) modulated the high-latitude ENSO response [*Carvalho et al.*, 2005; *Fogt and Bromwich*, 2006; *L'Heureux and Thompson*, 2006] and contributed to the observed decadal variability in both ENSO and SAM.

5. Ice-Atmosphere Spatial Variability

[32] The spatial variability of ice-atmosphere interactions during the austral autumn advance was investigated next in relation to ENSO and SAM variability to better understand why trends were detected in only the wAP/sBS and wRS regions. Our approach was to compute composites (averages) of MAM SLP and sea ice advance anomalies as follows: (1) 1980s El Niños (N = 2) and La Niñas (N = 3) versus the 1990s El Niños (N = 2) and La Niñas (N = 3) (Figure 6, Table 3), and (2) 1980s -SAM with and without coincident El Niño (N = 2 and N = 5, respectively) versus 1990s +SAM with and without coincident La Niña (N = 3 and N = 4, respectively) (Figure 7, Table 3). The composites included only those years with a normalized Niño 3.4/SAM index exceeding ±0.5 as listed in Table 3.

[33] Though ideally we would like to be able to distinguish ice-atmosphere anomalies associated with just the high-latitude response to ENSO versus the response to SAM, this was not possible given the relatively short time period and high variability, as well as the prevailing influence of -SAM in the 1980s versus +SAM in the 1990s. We therefore emphasize the exploratory nature of this analysis, the results of which can only be suggestive, given the small sample sizes and relatively high variability. Nonetheless, the approach outlined above helped to resolve where and when decadal changes in regional ice-atmosphere anomalies were most distinct, thus helping to explain why strong sea ice trends were detected in the wAP/sBS and wRS regions and not elsewhere in the Southern Ocean.

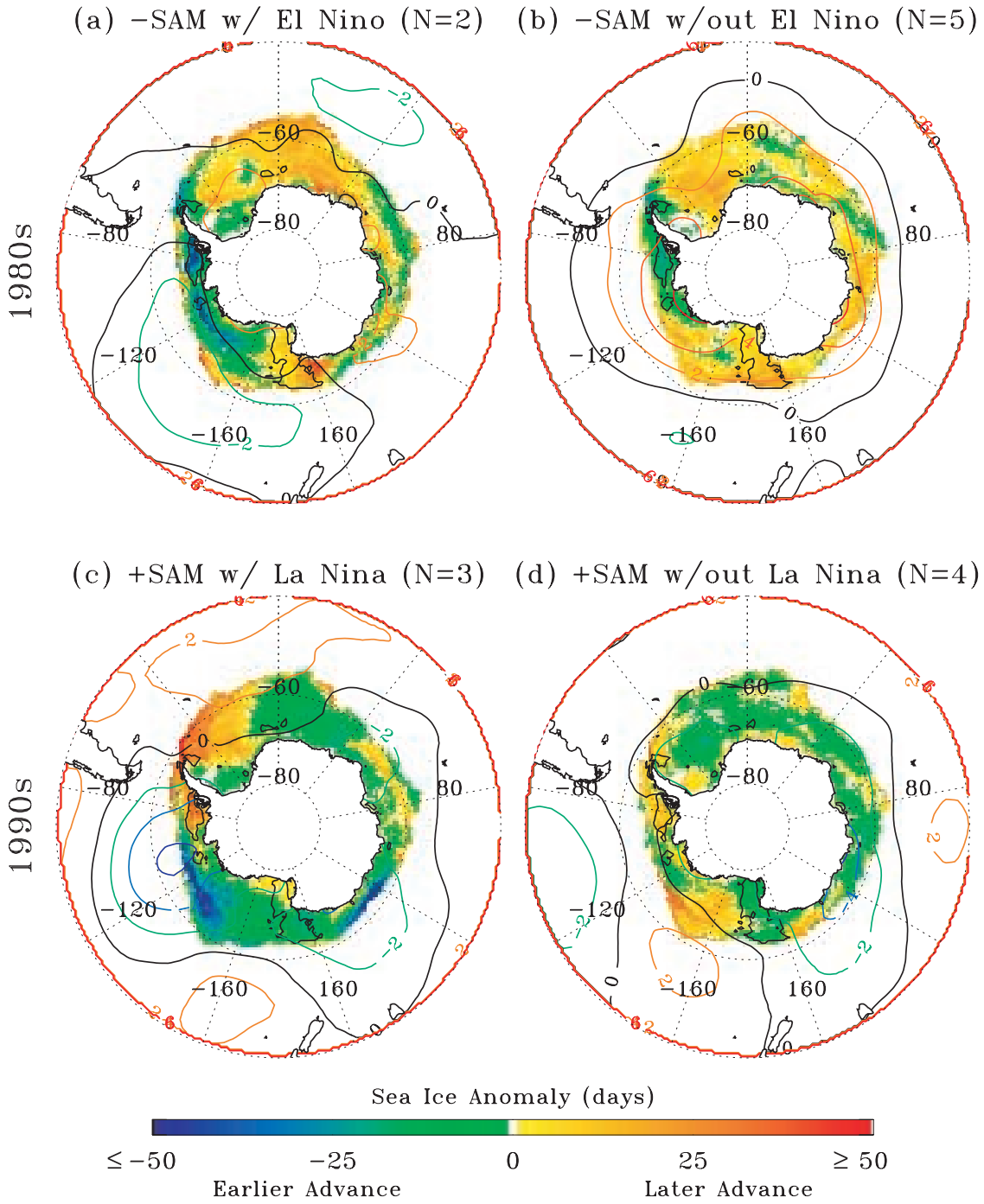

Figure 7. SAM composites of sea ice advance (color shading) and MAM SLP (color contours) anomalies for (a) 1980s -SAMs coincident with El Niño (N = 2), (b) 1980s −SAMs not coincident with El Niño (N = 5), (c) 1990s +SAMs coincident with La Niña (N = 3), and (d) 1990s +SAMs not coincident with La Niña (N = 4). See Table 3 for list of SAM years used. Figures 7a and 7c are the same as Figures 6a and 6d, respectively, reproduced here for ease of comparison. See Table 4 for mean regional sea ice advance anomalies for each composite shown in Figure 7.

5.1. Composites of 1980s Versus 1990s ENSOs

[34] The El Niño and La Niña composites (Figure 6) for the 1980s versus the 1990s highlight the variability in the high-latitude response to El Niño in particular as well as decadal changes in general. The canonical high-latitude atmospheric response to the 1980s El Niños (e.g., positive SLP anomalies at high latitudes in the South Pacific) was not present in MAM (Figure 6a). However, and contrary to the SLP anomalies, the sea ice advance anomalies for the 1980s El Niños suggest positive, not negative, SLP anomalies centered roughly on 160°W (i.e., with cold southerly winds east of 160°W promoting an early sea ice advance).

[35] In contrast, the high-latitude ice-atmosphere response for the 1990s El Niños (Figure 6c) was more consistently canonical, showing strong positive SLP anomalies centered on 90°W, together with an Antarctic Dipole pattern in the sea ice advance anomaly. It should be noted that the ice-atmosphere anomaly pattern in Figure 6c was strongly influenced by the 1992 El Niño in particular, which was coincident with a strong -SAM (whereas the 1998 El Niño was coincident with a strong +SAM, showing similar but weaker ice-atmosphere anomalies compared to the 1992 El Niño).

[36] The distinctly different sea ice anomaly patterns for the 1980s versus 1990s El Niño composites (Figures 6a and 6c) also showed anomalies switching sign between the 1980s and 1990s El Niños in some regions, for example, from mostly positive to negative in the Weddell Sea (between 40°W and 0°E) and from mostly negative to positive in the western Bellingshausen, Amundsen and eastern Ross Seas. These decadal changes in the high-latitude response to El Niño appear to be consistent with other observations of a significant weakening or phase reversal between ENSO and West Antarctic precipitation covariability reported to have occurred around 1990 [*Cullather et al.*, 1996; *Bromwich et al.*, 2000; *Genthon and Cosme*, 2003].

[37] In contrast to the El Niño composites, the MAM SLP and sea ice advance anomalies for La Niña showed similar patterns between the 1980s (Figure 6b) and 1990s (Figure 6d), though were of higher magnitude in the 1990s particularly between 40°W and 160°W. As shown in Table 3, all three of the 1990s La Niñas coincided with strong +SAM, whereas for the other three composites (Figures 6a–6c) the mean absolute magnitudes of the coincident SAMs were not as high (e.g., 1980s El Niño) or of mixed sign (1980s La Niña and 1990s El Niño). Consistent with *Fogt and Bromwich* [2006] these results indicate that when ENSO and SAM strongly and constructively covaried (e.g., La Niña with +SAM, and vice versa), the SLP anomalies strengthened poleward and/or eastward (compared to other ENSOs). In turn, the sea ice anomalies also were stronger and more spatially coherent with the SLP anomalies.

5.2. Composites of 1980s -SAMs Versus 1990s +SAMs

[38] We next compared composites of 1980s -SAMs with and without coincident El Niños (N = 2 and N = 5, respectively, Figures 7a and 7b) and composites of 1990s +SAMs with and without coincident La Niñas (N = 3 and N = 4, respectively, Figures 7c and 7d) to investigate the prevailing influence of -SAM in the 1980s versus +SAM in the 1990s. Note that Figures 7a (1980s -SAM coincident with El Niño) and 7c (1990s +SAM coincident with La Niña) are the same as Figures 6a and 6d, reproduced here for ease of comparison.

[39] Interestingly, the canonical high-latitude ice-atmosphere anomaly pattern for SAM (see Figure 1) was best illustrated for the 1980s -SAM not coincident with El Niño (Figure 7b) and for the 1990s +SAM coincident with La Niña (Figure 7c). A canonical ice-atmosphere response to SAM is interpreted as follows. Under negative SAM conditions (e.g., Figures 7a and 7b) westerly winds are expected to be weaker. In turn, the weaker westerly winds mean weaker Ekman sea ice drift to the north, and therefore average to late sea ice advance. The exception would be the region under the influence of more southwesterly winds (e.g., the eastern limb of the positive pressure anomaly centered on ~120°W in Figure 7b), where Ekman sea ice drift would be to the northeast and would help to promote an early sea ice advance.

[40] In contrast, under positive SAM conditions (e.g., Figures 7c and 7d) the expectation would be for stronger, more poleward westerly winds, thus stronger Ekman sea ice drift to the north and early sea ice advance everywhere, except in the region under the influence of more northeasterly winds (e.g., the eastern limb of the negative pressure anomaly centered on ~110°W in Figure 7c), which would help to inhibit sea ice advance. Though the canonical ice-atmosphere anomaly pattern for SAM was best illustrated for the 1980s -SAM not coincident with El Niño (Figure 7b) and for the 1990s +SAM coincident with La Niña (Figure 7c), the SAM-like annular signature was detectable in the sea ice anomalies in all four composites, though the area showing a nonannular component changed in longitude/magnitude (Figures 7c and 7d) and/or spatial extent (Figure 7a versus Figure 7b).

[41] For each of the composites shown in Figure 7, the mean regional sea ice advance anomalies (for the wAP/sBS and wRS regions) are listed in Table 4. Also shown in Table 4 are the mean decadal sea ice advance anomalies for the -SAMs during 1980 to 1990 (N = 7) and the +SAMs during1991 to 2000 (N = 7). Though the SAM sea ice anomalies were generally of lesser magnitude than the SAM/ENSO sea ice anomalies, particularly in the wAP/sBS region, the SAM sea ice anomalies nonetheless contributed to the consistency of the decadal sea ice changes observed in the wAP/sBS and wRS regions.

[42] Spatial maps of decadal anomaly differences further highlight the consistency, or lack thereof, of the regional sea ice response to SAM/ENSO (Figure 8a) and SAM (Figure 8b). Sea ice anomaly differences in the wAP/sBS and wRS regions between the 1980s and 1990s showed strong and consistent (same sign) anomaly responses during both SAM/ENSO and SAM. This also was true for some areas in the central/eastern Weddell Sea (between 20°W and 40°E) and along East Antarctica (between 90°E and 130°E). However, strong regional trends were not detected in those other areas owing to overall higher sea ice variability over 1979–2004 that weakened trend significance (Figure 4). Outside these consistently responding regions, anomaly differences between the 1980s and 1990s were weaker or of different sign for SAM/ENSO versus SAM sea ice anomalies (e.g., the western Weddell, Amundsen and eastern Ross Sea regions), most likely a result of decadal variability in the high-latitude response to El Niño in particular (as discussed in reference to Figures 6a and 6c). In section 6.1 we provide further discussion of how ENSO/SAM-related variability, particularly as related to wind-driven sea ice anomalies, contributed to the regional ice-atmosphere anomaly patterns shown in Figures 6–8.

[43] We now compare our results to those of *Liu et al.* [2004] who suggested that ENSO and SAM variability could only explain a fractional amount of the regional sea ice trends, and that other large-scale processes and/or local feedbacks must be contributing to the regional sea ice trends. Recall, the regional trends detected in ice season duration (Figure 4c) were spatially similar to those detected

Table 4. Mean Regional Sea Ice Advance Anomalies for the Composites Shown in Figure 7[a]

	wAP/sBS Mean ± Std (days)	wRS Mean ± Std (days)
Figure 7		
(a) 1980s −SAM w/El Niño (N = 2)	−28.2 ± 17.3	+10.2 ± 7.8
(b) 1980s -SAM w/out El Niño (N = 5)	−15.1 ± 8.0	+12.2 ± 7.5
(c) 1990s +SAM w/La Niña (N = 3)	+22.3 ± 14.5	−7.8 ± 7.9
(d) 1990s +SAM w/out La Niña (N = 4)	+9.7 ± 8.6	− 4.7 ± 4.8
Decadal Means		
-SAM, 1980 to 1990 (N = 7)	−18.8 ± 9.1	+11.5 ± 6.6
+SAM, 1991 to 2000 (N = 7)	+15.0 ± 9.4	−6.0 ± 4.5

[a]A negative advance anomaly means the advance was earlier (with respect to the mean day of advance), whereas a positive advance anomaly means the advance was later.

by *Liu et al.* [2004] using monthly sea ice concentration. We first suggest that analyzing monthly sea ice concentrations for climate signals is problematic, since the sensitivity of the sea ice response to changes in atmospheric circulation varies most notably between the physical mechanics of sea ice advance and retreat, which in turn vary between inner and outer pack ice regions. Thus, there are different ice-climate sensitivities at different times of the year. We also note that the decadal variability in the high-latitude ENSO response, in conjunction with a change in the mean state of SAM, produced different ENSO- and SAM-related ice-atmosphere anomaly patterns between the 1980s and 1990s. Therefore, linear correlations between monthly sea ice concentrations and ENSO and SAM variability over 1979–2004 as computed by *Liu et al.* [2004] will be weakened by the observed decadal changes and seasonally varying ice-climate sensitivities.

[44] Further, there is the observation that the high-latitude ice-atmosphere response to El Niño significantly changed between the 1980s and 1990s (e.g., Figures 6a and 6c) and that the response to positive and negative SAM/ENSO is not spatially (inversely) symmetric (e.g., Figures 7a and 7c). However, we agree with *Liu et al.* [2004] in that other large-scale processes (e.g., the high-latitude response to global warming, ozone depletion inducing a positive SAM) and/or local feedbacks also contributed to the regional sea ice trends. (See section 6.2 for further discussion of possible large-scale processes and local feedbacks.) Nonetheless, when we focused our analysis on sea ice advance and resolved the mean sea ice response to the 1980s -SAMs (with and without coincident El Niños) versus the 1990s +SAMs (with and without coincident La Niñas), we were able to explain why there were regional sea ice trends in the wAP/sBS and wRS regions and not elsewhere in the Southern Ocean.

6. Discussion

6.1. Regional Changes in the Wind-Driven Sea Ice Response

[45] The southeastward strengthening of negative SLP anomalies in the South Pacific in the 1990s in association

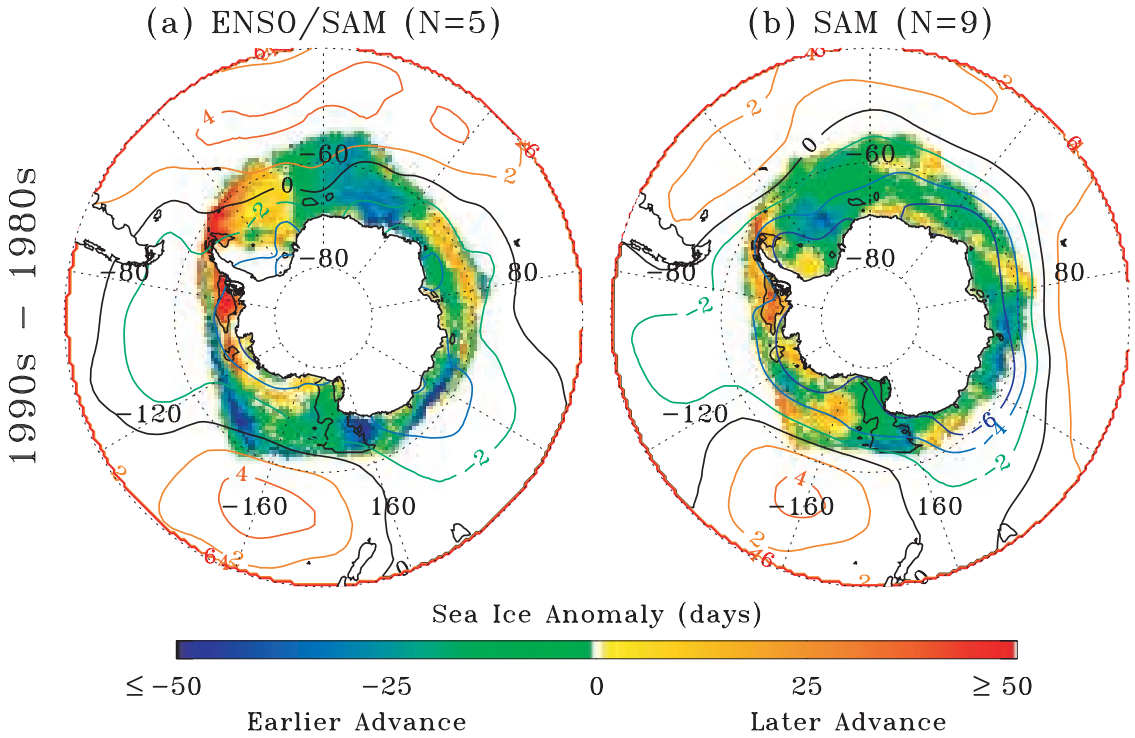

Figure 8. Decadal composite differences (1990s minus 1980s) of sea ice advance (color shading) and MAM SLP (color contours) anomalies for (a) 1990s +SAM/La Niña minus 1980s -SAM/El Niño (N = 5, Figure 7c minus 7a), and (b) 1990s +SAM minus 1980s -SAM (N = 9, Figure 7d minus 7b). See Table 3 for list of SAM years used.

with +SAMs (particularly those coincident with La Niñas) help to explain changes in the wind-driven sea ice response in the wAP/sBS region. With the southeastward intensification (toward the Antarctic Peninsula) of negative SLP anomalies during spring-autumn, strong northerly winds intensified over the wAP/sBS region, promoting a more extensive sea ice retreat (poleward) in spring-summer followed by subsequent delays in the sea ice advance in autumn (changes in SLP and winds are further substantiated below). The near complete removal of summer sea ice in the southern Bellingshausen Sea in 1988–1989 and 1998–1999 leaves little doubt of the magnitude of the impact from +SAMs coincident with La Niñas.

[46] The intensification of northerly winds in the 1990s is consistent with the findings of *Massom et al.* [2008] who found a per annum increase in wind speed of ~0.20 m/s from 1990 to 2005 during the month of September in the vicinity of 70°S, 90°W, with highest wind speeds from the north. We also calculated the trends in the NNR winds using seasonal averages of the zonal and meridional components and found negative trends in the meridional winds (i.e., trends toward more northerly winds) in the wAP/sBS region (in the vicinity of 68°S, 83°W) in all seasons in the 1980s. The strongest trends were during SON (-0.28 ± 0.08 m/s) and MAM (-0.21 ± 0.15 m/s), and these continued into the 1990s (SON: -0.11 ± 0.21 m/s; MAM: -0.18 ± 0.15 m/s). The detection of trends in seasonal averages of winds is suggestive and consistent with the large-scale changes in NNR SLP data, as well as SLP changes as measured at Rothera Station (67.5°S, 68.1°W), which show decreases in DJF and MAM SLP of -0.10 ± 0.12 and -0.03 ± 0.16 mbar/a over 1979–2004, respectively. Additionally, the seasonal trends in winds may well be conservative estimates, given that the NNR wind data typically underestimate strong wind events [*Yuan*, 2004b], which as previous studies have shown, can effect significant changes in ice edge location [e.g., *Stammerjohn et al.*, 2003; *Turner et al.*, 2003; *Harangozo*, 2004a, 2006; *Massom et al.*, 2006, 2008].

[47] In addition, the eastward strengthening of the SLP anomalies in the 1990s in association with ENSO in particular (e.g., Table 2 and Figures 6c and 6d) also helps to explain the phase reversal of the ENSO-related sea ice anomalies in western Weddell, Amundsen and eastern Ross Seas, consistent with previous observations of a significant weakening or phase reversal between ENSO and West Antarctic precipitation covariability reported to have occurred around 1990 [*Cullather et al.*, 1996; *Bromwich et al.*, 2000; *Genthon and Cosme*, 2003]. For example, in the Amundsen Sea (and to some extent the eastern Ross Sea), the ENSO-related meridional wind component switched sign as the center of the SLP anomalies strengthened from west to east over this region. Consequently, in the 1990s the Amundsen Sea came more under the influence of the western limb of the SLP anomalies (thus cold southerly winds during La Niña) versus being more under the influence of the eastern limb (warm northerly winds during La Niña) in the 1980s. This is indicated by correlations between MAM Niño 3.4 index and the NNR meridional winds in the vicinity of 68°S, 130°W, which switched sign between the 1980s ($R = +0.66$, thus northerly winds during La Niña) and the 1990s ($R = -0.71$, thus southerly winds during La Niña). In contrast, in the western Weddell Sea correlations between the DJF Niño 3.4 index and the NNR meridional winds in the vicinity of 68°S, 40°W switched sign in the opposite direction between the 1980s ($R = -0.42$, thus southerly winds during La Niña) and 1990s ($R = +0.75$, thus northerly winds during La Niña).

[48] In contrast, the switch from a more negative SAM in the 1980s to a more positive SAM in the 1990s strongly influenced ice-atmosphere interactions in the wRS region, whereas the ENSO-related changes between the 1980s and 1990s defy the designation of a typical ENSO response in this region. The strengthened westerly winds in the 1990s helped to delay sea ice retreat (via Ekman drift to the north) as well as helped to accelerate sea ice advance, whereas in the 1980s when westerly winds were on average weaker, the sea ice retreat was earlier, advance later. This is consistent with seasonal MAM trends detected in the NNR zonal wind data in the vicinity of 66°S, 173°E, which switched from a very weak easterly wind trend in the 1980s (-0.02 ± 0.23 m/s) to a westerly wind trend in the 1990s ($+0.37 \pm 0.41$ m/s). Also, the overall intensification of the atmospheric circulation in the South Pacific during La Niña and/or +SAM events likely strengthened the Ross Sea gyre (and perhaps katabatic wind flow off the Ross Ice Shelf). This too is consistent with the seasonal SON trends detected in the NNR meridional winds (in the same vicinity as above), which switched from a northerly wind trend in the 1980s (-0.21 ± 0.15 m/s) to a southerly wind trend in the 1990s ($+0.17 \pm 0.11$ m/s). The strengthening of these factors would contribute a constant northward flow of sea ice from the southern Ross Sea, thus helping to explain the continuity of trends between the southwestern and northwestern Ross Sea regions.

6.2. Climate Change in the Antarctic Peninsula Region and Hemispheric Climate Mechanisms

[49] As summarized by *Stammerjohn et al.* [2008] the ocean-atmosphere-ice interactions and trends in the wAP/sBS region are consistent with the overall rapid regional warming of the AP region. For example, the strong trend toward a later autumn sea ice advance is associated with increased northerly winds (as described above), which advect warm air into the region from lower latitudes, and which inhibit sea ice from advancing, thus also facilitating increased ocean heat flux to the overlying atmosphere in autumn. In addition, increased upwelling of warm Upper Circumpolar Deep Waters onto the wAP shelf, in response to increased storminess, has been associated with strong increases in ocean heat content on the shelf [*Martinson et al.*, 2008]. Finally, the trend toward a shorter sea ice season is concurrent with a decreasing trend in monthly sea ice concentration [*Liu et al.*, 2004] and an increase in intraseasonal sea ice variability (as described in the Introduction), changes that suggest relatively thinner sea ice and/or increased lead fraction, either of which increase ocean heat flux to the atmosphere throughout winter. Together, these seasonal sea ice-mediated changes would contribute to, or amplify, warming in the AP region in autumn/early winter as suggested by others [e.g., *Kwok and Comiso*, 2002b; *Vaughan et al.*, 2003; *Meredith and King*, 2005; *Harangozo*, 2006].

[50] The timing of sea ice advance and retreat is strongly coupled to the location and intensity of the circumpolar trough (a surface low-pressure belt between 60°S and 70°S),

which in the South Pacific is linked to the southern component of the "split jet," the polar front jet stream (Figure 1). Ultimately the location and intensity of the polar front jet is determined by the meridional temperature gradient in the South Pacific. Seasonally, the meridional temperature gradient at mid-to-high latitudes strengthens during spring and autumn and weakens during summer and winter, respectively, in accord with the SAO [*van Loon*, 1967] as described in the Introduction. However, the SAO, and thus sea ice advance and retreat, can be modulated by any natural or anthropogenic perturbation that affects the meridional temperature gradient (e.g., ENSO, SAM, ozone depletion, increasing greenhouse gases).

[51] The primary mechanisms for SAM and ENSO to affect sea ice would be via wind-driven advection of heat, moisture and momentum, and this implies an impact on the SLP field associated with these modes of variability. The more positive phase dominance of the SAM in recent decades has been related to both CO_2 increases [*Fyfe et al.*, 1999; *Kushner et al.*, 2001; *Marshall et al.*, 2004; *Shindell and Schmidt*, 2004] and stratospheric ozone depletion [*Thompson and Solomon*, 2002; *Gillet and Thompson*, 2003]: each leads to increased latitudinal temperature gradients at higher levels in the troposphere, with associated westerly wind increases. The stronger west winds then refract planetary waves preferentially equatorward, providing angular momentum transport toward the pole, helping to sustain the stronger west winds and lower pressure at high-latitude regions.

[52] Further, as shown by *Marshall et al.* [2004], the positive trend in SAM could not be reproduced in model simulations using only natural forcings but was reproduced (most notably the large positive trend in summer) when both natural and anthropogenic forcings were used. These authors note however that since the trend in SAM began prior to ozone depletion, and since the trends are strongest in summer-autumn, increasing greenhouse gases, when acting in combination with natural forcings, appear to be the dominant process producing the positive trend in SAM. This study in particular emphasizes the SAM-related ice-atmosphere changes in austral autumn (March-April-May) and the associated and significant impacts on regional sea ice trends, which are unlikely owing to ozone-related changes during austral spring. Additionally, there is the suggestion that changes in summer sea ice extent could feedback on SAM variability. For example, *Raphael* [2003] shows that a net decrease in the overall retention of sea ice during spring-autumn (as Table 1 indicates) could potentially reinforce +SAM conditions.

[53] ENSO phenomena also affect the latitudinal temperature gradient in the respective oceans basins [e.g., *Rind et al.*, 2001], thus also impact the wind field and planetary wave propagation. It is important to note that even for El Niño events, different patterns of SST warming and atmospheric convection in the tropical Pacific lead to somewhat different zonal wind structures [*Cess et al.*, 2001], varying Rossby wave generation [e.g., *Harangozo*, 2004b; *Lachlan-Cope and Connolley*, 2006], and very different latitudinal temperature gradients in the troposphere [*Trenberth and Smith*, 2006]. Each particular zonal wind pattern will have its own influence on planetary wave propagation (in an interactive way) and hence SLP patterns. The combination, then, of positive or negative SAMs and particular El Niño or La Niña sea surface temperature anomalies will produce different SLP responses and sea ice advection. In a subsequent paper we will discuss in greater detail how the resulting sea ice variability patterns compare to planetary wave generation and propagation changes associated with these modes of climate variability, as well as possible local responses that might be affecting the sea ice response.

[54] With continued greenhouse gas increases, it is predicted that the positive trend in SAM in summer and autumn will continue [e.g., *Marshall et al.*, 2004] with perhaps some mitigation by ozone recovery [e.g., *Shindell and Schmidt*, 2004], though it is unclear how springtime changes induced by ozone recovery will affect summer and autumn SAM trends. Additionally, mitigation could come from changes in the intensity of atmospheric perturbations associated with potentially more intense El Niños in a warmer world, though the AR4 model studies were inconclusive with respect to future changes in El Niño [*Meehl et al.*, 2007]. If the positive trend in SAM continues, there may be regional ocean-atmosphere-ice feedbacks that reinforce the +SAM state and weaken any influence from the tropics. If such becomes the case, with time the sea ice trends in the western Weddell Sea would become consistent with those in the wAP/sBS region (earlier spring retreat, later autumn advance, decreasing ice season duration), whereas sea ice trends in the Amundsen and eastern Ross Seas would become consistent with those in the wRS region (later spring retreat, earlier autumn advance, increasing ice season duration), if current ice-climate relationships hold into the future. Finally, there is the additional potential that the interseasonal ice-ocean feedbacks will continue to enhance the winter warming in the Antarctic Peninsula. This in turn would continue to exacerbate the rapid retreat of marine glaciers and ice shelves in this region. There already is concern that the current retreat of glaciers and ice shelves is accelerating the flow and thinning of West Antarctic ice streams [e.g., *Payne et al.*, 2004; *Rignot et al.*, 2005]. Therefore, if regional warming of the Antarctic Peninsula continues, mass ice loss from the West Antarctic ice sheet is expected to increase, thus becoming a potentially significant contributor to future sea level rise.

7. Summary

[55] Our analysis indicated that variability and trends over 1979–2004 in the timing of the spring-summer sea ice retreat and subsequent autumn-winter sea ice advance determined variability and trends in ice season duration. Therefore, to understand why some regions show strong 26-year trends in ice season duration when other regions do not, we examined possible underlying causes that could create large regional anomalies in the timing of sea ice retreat and advance. Our key findings are as follows.

[56] 1. Over 1979–2004, sea ice retreated 31 ± 10 days earlier and advanced 54 ± 9 days later in the Antarctic Peninsula and southern Bellingshausen Sea (wAP/sBS) region, resulting in a decrease of 85 ± 20 ice season days. In the western Ross Sea (wRS) region, opposite trends were detected: sea ice retreated 29 ± 6 days later and advanced 31 ± 6 days earlier, resulting in an increase of 60 ± 10 ice season days.

[57] 2. Sea ice advance in most regions of the Southern Ocean was more highly correlated to ice season duration than sea ice retreat. Additionally, time series of sea ice advance, rather than of sea ice retreat, showed stronger covariability with seasonal time series of SLP, Niño 3.4 and SAM in the high-trending regions, particularly when the 1980s and 1990s were tested separately. In short, sea ice advance appeared to be more sensitive to climate variability than sea ice retreat, perhaps owing to its unconstrained equatorward expansion and ability to quickly respond to changing atmospheric conditions.

[58] 3. In general, ENSO- and SAM-related SLP anomalies at high latitudes in the South Pacific were centered between 130°W and 90°W and were negative during La Niña and/or +SAM and positive during El Niño and/or -SAM. However, the high-latitude response to ENSO was most pronounced when La Niña was coincident with +SAM and El Niño was coincident with -SAM (similar to the findings by *Fogt and Bromwich* [2006]), though the converse was not necessarily true. For example, strong ice-atmosphere anomalies occurred during -SAMs that were not coincident with El Niño.

[59] 4. There was an overall southeastward strengthening (toward the Antarctic Peninsula) of ENSO-related SLP anomalies over austral summer (DJF) and autumn (MAM) between the 1980s and 1990s, while SAM went from being mostly negative to mostly positive. In turn, region*al* trends in sea ice advance were consistent with the decadal changes in ice-atmosphere anomalies associated with: (1) the 1980s -SAMs that were coincident with El Niño (N = 2) and that were not coincident with El Niño (N = 5), and (2) the 1990s +SAMs that were coincident with La Niña (N = 3) and that were not coincident with La Niña (N = 4). In total, the 7 of 11 -SAMs between 1980 and 1990 and the 7 of 10 +SAMs between 1991 and 2000 were associated with distinct sea ice changes in the wAP/sBS region where *mean* sea ice advance was ~19 days earlier during the 1980s -SAMs and ~15 days later during the 1990s +SAMs, and in the wRS region, ~12 days later and ~6 days earlier, respectively. Elsewhere decadal sea ice changes were not as strong or sea ice variability was high (over 1979–2004), helping to explain why there were (opposing) sea ice trends in just the wAP/sBS and wRS regions and not elsewhere in the Southern Ocean.

[60] 5. The regional sea ice trends largely resulted from wind-driven sea ice changes. The deepening and southeastward strengthening of negative sea level pressure anomalies toward the Antarctic Peninsula in the 1990s in association with increasing +SAM and several coincident strong La Niñas, strengthened northerly winds in the wAP/sBS region during autumn-spring, leading to an earlier wind-driven sea ice retreat and later sea ice advance.

[61] 6. In the wRS region the strengthening of the zonal circulation in association with increasing +SAM in the 1990s created stronger westerly winds and more persistent northward Ekman sea ice drift, leading to a later wind-driven spring sea ice retreat and earlier autumn advance. In contrast, the weaker westerly winds in the 1980s in association with -SAMs created weaker wind-driven sea ice drift to the north in the wRS region, thus earlier sea ice retreats and later sea ice advances relative to the 1990s.

[62] Continued greenhouse gas increases would suggest a more +SAM. Thus, there may be a continuation, and perhaps spatial expansion, of the regional sea ice trends described here. If the trends in the wAP/sBS continue, then thinning of the West Antarctic ice sheet will likely continue, exacerbating sea level rise. In a subsequent paper we will investigate the potential mechanisms and sensitivities involved in the interactions between the high-latitude response to ENSO and SAM variability, with hopes of better understanding and predicting the ocean-atmosphere-ice response to climate change.

[63] **Acknowledgments.** This work was largely supported by a NASA Fellowship grant NGT5-30391 and leveraged by National Ocean and Atmosphere Administration grant/cooperative agreement NA17RJ1231 (S.E.S.), as well as by Palmer LTER NSF/OPP 0217282 (D.G.M., R.C.S., S.E.S.), NSF/OPP 0230284 (X.Y.), and the NASA Cryosphere Program (D.R.). The paper was finalized with support from the NOAA Climate and Global Change Postdoctoral Fellowship Program administered by the University Corporation for Atmospheric Research and conducted at the NASA Goddard Institute of Space Studies (S.E.S.). The 1979–2004 SMMR-SSM/I sea ice concentration data were from the EOS Distributed Active Archive Center (DAAC) at the National Snow and Ice Data Center, University of Colorado in Boulder, Colorado (http://nsidc.org). The sea level pressure data were from the National Center for Environmental Prediction/National Center for Atmospheric Research (NCEP/NCAR) Reanalysis Project. We thank Gareth Marshall for the SAM index data (http://www.nerc-bas.ac.uk/icd/gjma/sam.html), and the International Research Institute for Climate Prediction for the Niño 3.4 index data (http://iridl.ldeo.columbia.edu/). Finally, the authors are indebted to two excellent anonymous reviewers for their enduring attentiveness. This is Palmer LTER contribution 0299, and LDEO contribution 7104.

References

Bromwich, D. H., and R. L. Fogt (2004), Strong trends in the skill of the ERA-40 and NCEP-NCAR reanalyses in the high and middle latitudes of the Southern Hemisphere, 1958–2001, *J. Clim.*, *17*, 4603–4619.

Bromwich, D. H., A. N. Rogers, P. Kallberg, R. I. Cullather, J. W. C. White, and K. J. Kreutz (2000), ECMWF analyses and reanalyses depiction of ENSO signal in Antarctic precipitation, *J. Clim.*, *13*, 1406–1420.

Cane, M. A., S. E. Zebiak, and S. C. Dolan (1986), Experimental forecasts of El Niño, *Nature*, *322*, 827–832.

Carvalho, L. M. V., C. Jones, and T. Ambrizzi (2005), Opposite phases of the Antarctic Oscillation and relationships with intraseasonal to interannual activity in the tropics during austral summer, *J. Clim.*, *18*, 702–718.

Cess, R. D., M. Zhang, P.-H. Wang, and B. A. Wielicki (2001), Cloud structure anomalies over the tropical Pacific during the 1997/98 El Niño, *Geophys. Res. Lett.*, *28*(24), 4547–4550.

Comiso, J. C. (1995), Sea-ice geophysical parameters from SMMR and SSM/I data, in *Oceanographic Applications of Remote Sensing*, edited by M. Ikeda and F. Dobson, pp. 321–338, CRC Press, Boca Raton, Fla.

Comiso, J. C., D. Cavalieri, C. Parkinson, and P. Gloersen (1997), Passive microwave algorithms for sea ice concentration—A comparison of two techniques, *Remote Sens. Environ.*, *60*(3), 357–384.

Connolley, W. M., and S. A. Harangozo (2001), A comparison of five numerical weather prediction analysis climatologies in southern high latitudes, *J. Clim.*, *14*, 30–44.

Cook, A. J., A. J. Fox, D. G. Vaughan, and J. G. Ferrigno (2005), Retreating glacier fronts on the Antarctic Peninsula over the past half-century, *Science*, *308*, 541–544.

Cullather, R. I., D. H. Bromwich, and M. L. Van Woert (1996), Interannual variations in Antarctic precipitation related to El Niño Oscillation, *J. Geophys. Res.*, *101*(D14), 19,109–19,118.

Domack, E., A. Leventer, A. Burnett, R. Bindschadler, P. Convey, and M. Kirby (2003), *Antarctic Peninsula Climate Variability: Historical and Paleoenvironmental Perspectives*, *Antarct. Res. Ser.*, vol. 79, edited by E. Domack et al., AGU, Washington, D. C.

Drinkwater, M. R., R. Kwok, C. A. Geiger, J. A. Maslanik, C. W. Fowler, and W. J. Emery (1999), Quantifying surface fluxes in the ice-covered polar oceans using satellite microwave remote sensing data, paper presented at Ocean Observing System for Climate (OceanObs'99), Cent. Natl. Etudes Spatiales, San Raphael, France.

Enomoto, H., and A. Ohmura (1990), Influences of atmospheric half-yearly cycle on the sea ice extent in the Antarctic, *J. Geophys. Res.*, *95*(C6), 9497–9511.

Fogt, R. L., and D. H. Bromwich (2006), Decadal variability of the ENSO teleconnection to the high latitude South Pacific governed by coupling with the Southern Annular Mode, *J. Clim.*, *19*, 979–997.

Fyfe, J. C., G. J. Boer, and G. M. Flato (1999), The Arctic and Antarctic Oscillations and their projected changes under global warming, *Geophys. Res. Lett.*, *26*(11), 1601–1604.

Genthon, C., and E. Cosme (2003), Intermittent signature of ENSO in west-Antarctic precipitation, *Geophys. Res. Lett.*, *30*(21), 2081, doi:10.1029/2003GL018280.

Gillet, N. P., and D. W. J. Thompson (2003), Simulation of recent Southern Hemisphere climate change, *Science*, *302*, 273–275.

Gloersen, P. (1995), Modulation of hemispheric sea-ice cover by ENSO events, *Nature*, *373*, 503–506.

Gloersen, P., W. J. Campbell, D. J. Cavalieri, J. C. Comiso, C. L. Parkinson, and H. J. Zwally (1992), *Arctic and Antarctic Sea Ice, 1978–1987: Satellite Passive-Microwave Observations and Analysis*, NASA, Washington, D. C.

Gong, D., and S. Wang (1999), Definition of Antarctic oscillation index, *Geophys. Res. Lett.*, *26*(4), 459–462.

Hall, A., and M. Visbeck (2002), Synchronous variability in the Southern Hemisphere atmosphere, sea ice and ocean resulting from the Annular Mode, *J. Clim.*, *15*, 3043–3057.

Harangozo, S. A. (2000), A search for ENSO teleconnections in the west Antarctic Peninsula climate in austral winter, *Int. J. Climatol.*, *20*, 663–679.

Harangozo, S. A. (2004a), The impact of winter ice retreat on Antarctic winter sea-ice extent and links to the atmospheric meridional circulation, *Int. J. Climatol.*, *24*, 1023–1044.

Harangozo, S. A. (2004b), The relationship of Pacific deep tropical convection to the winter and springtime extratropical atmospheric circulation of the South Pacific in El Niño events, *Geophys. Res. Lett.*, *31*, L05206, doi:10.1029/2003GL018667.

Harangozo, S. A. (2006), Atmospheric circulation impacts on winter maximum sea ice extent in the west Antarctic Peninsula region (1979–2001), *Geophys. Res. Lett.*, *33*, L02502, doi:10.1029/2005GL024978.

Jacobs, S. S., and J. C. Comiso (1997), Climate variability in the Amundsen and Bellingshausen Seas, *J. Clim.*, *10*, 697–709.

Kalnay, E., et al. (1996), The NCEP/NCAR 40-year reanalysis project, *Bull. Am. Meteorol. Soc.*, *77*, 437–471.

Kanamitsu, M., R. E. Kistler, and R. W. Reynolds (1997), NCEP/NCAR reanalysis and the use of satellite data, in *Satellite Data Applications: Weather and Climate*, edited by R. G. Ellingson, pp. 481–489, Pergamon, Oxford, U. K.

King, J. C. (2003), Validation of ECMWF sea level pressure analyses over the Bellingshausen Sea, Antarctica, *Weather Forecasting*, *18*, 536–540.

Kistler, R., et al. (2001), The NCEP-NCAR 50-year reanalysis: Monthly means CD-ROM and documentation, *Bull. Am. Meteorol. Soc.*, *82*, 247–267.

Kushner, P. J., I. M. Held, and T. L. Delworth (2001), Southern Hemisphere atmospheric circulation response to global warming, *J. Clim.*, *14*, 2238–2249.

Kwok, R., and J. C. Comiso (2002a), Southern Ocean climate and sea ice anomalies associated with the Southern Oscillation, *J. Clim.*, *15*, 487–501.

Kwok, R., and J. C. Comiso (2002b), Spatial patterns of variability in Antarctic surface temperature: Connections to the Southern Hemisphere Annular Mode and the Southern Oscillation, *Geophys. Res. Lett.*, *29*(14), 1705, doi:10.1029/2002GL015415.

Lachlan-Cope, T., and W. Connolley (2006), Teleconnections between the tropical Pacific and the Amundsen-Bellingshausen Sea: Role of the El Niño/Southern Oscillation, *J. Geophys. Res.*, *111*, D23101, doi:10.1029/2005JD006386.

Lefebvre, W., and H. Goosse (2005), Influence of the Southern Annular Mode on the sea ice-ocean system: The role of the thermal and mechanical forcing, *Ocean Sci.*, *1*, 145–157.

Lefebvre, W., H. Goosse, R. Timmermann, and T. Fichefet (2004), Influence of the Southern Annular Mode on the sea ice–ocean system, *J. Geophys. Res.*, *109*, C09005, doi:10.1029/2004JC002403.

L'Heureux, M. L., and D. W. J. Thompson (2006), Observed relationships between the El Niño–Southern Oscillation and the extratropical zonal-mean circulation, *J. Clim.*, *19*, 276–287.

Liu, J., X. Yuan, D. Rind, and D. G. Martinson (2002), Mechanism study of the ENSO and southern high latitude climate teleconnections, *Geophys. Res. Lett.*, *29*(14), 1679, doi:10.1029/2002GL015143.

Liu, J., J. A. Curry, and D. G. Martinson (2004), Interpretation of recent Antarctic sea ice variability, *Geophys. Res. Lett.*, *31*, L02205, doi:10.1029/2003GL018732.

Marshall, G. J. (2003), Trends in the Southern Annular Mode from observations and reanalyses, *J. Clim.*, *16*, 4134–4143.

Marshall, G. J., and S. A. Harangozo (2000), An appraisal of NCEP/NCAR reanalysis MSLP data viability for climate studies in the South Pacific, *Geophys. Res. Lett.*, *27*(19), 3057–3060.

Marshall, G. J., P. A. Stott, J. Turner, W. M. Connolley, J. C. King, and T. A. Lachlan-Cope (2004), Causes of exceptional atmospheric circulation changes in the Southern Hemisphere, *Geophys. Res. Lett.*, *31*, L14205, doi:10.1029/2004GL019952.

Marshall, G. J., A. Orr, N. P. M. van Lipzig, and J. C. King (2006), The impact of a changing Southern hemisphere annular mode on Antarctic Peninsula summer temperature, *J. Clim.*, *19*, 5388–5404.

Martinson, D. G., S. E. Stammerjohn, R. A. Iannuzzi, R. C. Smith, and M. Vernet (2008), Palmer, Antarctica, Long-Term Ecological Research program first twelve years: Physical oceanography, spatio-temporal variability, *Deep Sea Res., Part II*, in press.

Massom, R. A., et al. (2006), Extreme anomalous atmospheric circulation in the west Antarctic Peninsula region in austral spring and summer 2001/2, and its profound impact on sea ice and biota, *J. Clim.*, *19*, 3544–3571.

Massom, R. A., S. E. Stammerjohn, W. Lefebvre, S. A. Harangozo, N. Adams, T. Scambos, M. J. Pook, and C. Fowler (2008), West Antarctic Peninsula sea ice in 2005: Extreme compaction and ice edge retreat due to strong climate anomaly, *J. Geophys. Res*. in press.

Meehl, G. A., et al. (2007), Global climate projections, in *Climate Change 2007: The Physical Science Basis. Contribution of Working Group I to the Fourth Assessment Report of the Intergovernmental Panel on Climate Change*, edited by S. Solomon et al., pp. 747–845, Cambridge Univ. Press, Cambridge, U. K.

Meredith, M. P., and J. C. King (2005), Rapid climate change in the ocean west of the Antarctic Peninsula during the second half of the 20th century, *Geophys. Res. Lett.*, *32*, L19604, doi:10.1029/2005GL024042.

Mo, K. C., and M. Ghil (1987), Statistics and dynamics of persistent anomalies, *J. Atmos. Sci.*, *44*, 877–901.

Parkinson, C. L. (1994), Spatial patterns in the length of the sea ice season in the Southern Ocean, *J. Geophys. Res.*, *99*(C8), 16,327–16,339.

Parkinson, C. L. (2002), Trends in the length of the Southern Ocean sea ice season, 1979–1999, *Ann. Glaciol.*, *34*, 435–440.

Parkinson, C. L. (2004), Southern Ocean sea ice and its wider linkages: Insights revealed from models and observations, *Antarct. Sci.*, *16*(4), 387–400.

Payne, A., A. Vieli, A. P. Shepherd, D. J. Wingham, and E. Rignot (2004), Recent dramatic thinning of largest West Antarctic ice stream triggered by oceans, *Geophys. Res. Lett.*, *31*, L23401, doi:10.1029/2004GL021284.

Raphael, M. N. (2003), Impact of observed sea-ice concentration on the Southern Hemisphere extratropical atmospheric circulation in summer, *J. Geophys. Res.*, *108*(D22), 4687, doi:10.1029/2002JD003308.

Rignot, E., G. Casassa, S. Gogineni, P. Kanagaratnam, W. Krabill, H. Pritchard, A. Rivera, R. Thomas, J. Turner, and D. Vaughan (2005), Recent ice loss from the Fleming and other glaciers, Wordie Bay, West Antarctic Peninsula, *Geophys. Res. Lett.*, *32*, L07502, doi:10.1029/2004GL021947.

Rind, D., M. Chandler, J. Lerner, D. G. Martinson, and X. Yuan (2001), Climate response to basin-specific changes in latitudinal temperature gradients and implications for sea ice variability, *J. Geophys. Res.*, *106*(D17), 20,161–20,173.

Santer, B. D., T. M. L. Wigley, J. S. Boyle, D. J. Gaffen, J. J. Hnilo, D. Nychka, D. E. Parker, and K. E. Taylor (2000), Statistical significance of trends and trend differences in layer-average atmospheric temperature time series, *J. Geophys. Res.*, *105*(D6), 7337–7356.

Scambos, T., C. Hulbe, and M. Fahnestock (2003), Climate-induced ice shelf disintegration in the Antarctic Peninsula, in *Antarctic Peninsula Climate Variability: Historical and Paleoenvironmental Perspectives*, *Antarct. Res. Ser.*, vol. 79, edited by E. Domack et al., pp. 79–92, AGU, Washington, D. C.

Shindell, D. T., and G. A. Schmidt (2004), Southern Hemisphere climate response to ozone changes and greenhouse gas increases, *Geophys. Res. Lett.*, *31*, L18209, doi:10.1029/2004GL020724.

Silvestri, G. E., and C. S. Vera (2003), Antarctic Oscillation signal on precipitation anomalies over southeastern South America, *Geophys. Res. Lett.*, *30*(21), 2115, doi:10.1029/2003GL018277.

Simmonds, I., and J. C. King (2004), Global and hemispheric climate variations affecting the Southern Ocean, *Antarct. Sci.*, *16*(4), 401–413.

Smith, R. C., and S. E. Stammerjohn (2001), Variations of surface air temperature and sea ice extent in the western Antarctic Peninsula (WAP) region, *Ann. Glaciol.*, *33*, 493–500.

Smith, R. C., K. S. Baker, and S. E. Stammerjohn (1998), Exploring sea ice indexes for polar ecosystem studies, *BioScience*, *48*(2), 83–93.

Stammerjohn, S. E., and R. C. Smith (1997), Opposing Southern Ocean climate patterns as revealed by trends in regional sea ice coverage, *Clim. Change*, *37*(4), 617–639.

Stammerjohn, S. E., M. R. Drinkwater, R. C. Smith, and X. Liu (2003), Ice-atmosphere interactions during sea-ice advance and retreat in the western Antarctic Peninsula region, *J. Geophys. Res.*, *108*(C10), 3329, doi:10.1029/2002JC001543.

Stammerjohn, S. E., D. G. Martinson, R. C. Smith, and R. A. Iannuzzi (2008), Sea ice in the western Antarctic Peninsula region: Spatio-temporal variability from ecological and climate change perspectives, *Deep Sea Res., Part II*, in press.

Steffen, K., J. Key, D. J. Cavalieri, J. Comiso, P. Gloersen, K. M. S. Germain, and L. Rubinstein (1992), The estimation of geophysical parameters using passive microwave algorithms, in *Microwave Remote Sensing of Sea Ice*, *Geophys. Monogr. Ser.*, vol. 68, edited by F. Carsey, pp. 201–231, AGU, Washington, D. C.

Sturaro, G. (2003), A closer look at the climatological discontinuities present in the NCEP/NCAR reanalysis temperature due to the introduction of satellite data, *Clim. Dyn.*, *21*, 309–316.

Thompson, D. W. J., and S. Solomon (2002), Interpretation of recent Southern Hemisphere climate change, *Science*, *296*, 895–899.

Thompson, D. W. J., and J. M. Wallace (2000), Annual modes in the extratropical circulation, Part I: month-to-month variability, *J. Clim.*, *13*, 1000–1016.

Trenberth, K. E., and L. Smith (2006), The vertical structure of temperature in the tropics: Different flavors of El Niño, *J. Clim.*, *19*, 4956–4970.

Turner, J. (2004), Review: The El Niño–Southern Oscillation and Antarctica, *Int. J. Clim.*, *24*, 1–31.

Turner, J., S. A. Harangozo, J. C. King, W. M. Connolley, T. A. Lachlan-Cope, and G. J. Marshall (2003), An exceptional winter sea-ice retreat/advance in the Bellingshausen Sea, Antarctica, *Atmos. Ocean*, *41*(2), 171–185.

Turner, J., T. Lachlan-Cope, S. Colwell, and G. J. Marshall (2005), A positive trend in western Antarctic Peninsula precipitation over the last 50 years reflecting regional and Antarctic-wide atmospheric circulation changes, *Ann. Glaciol.*, *41*, 85–91.

van den Broeke, M. R. (2000), The semi-annual oscillation and Antarctic Climate. Part 4: A note on sea ice cover in the Amundsen and Bellingshausen Seas, *Int. J. Climatol.*, *20*, 455–462.

van Loon, H. (1967), The half-yearly oscillations in middle and high southern latitudes and the coreless winter, *J. Atmos. Sci.*, *24*(5), 472–486.

Vaughan, D. G., G. J. Marshall, W. M. Connolley, C. Parkinson, R. Mulvaney, D. A. Hodgson, J. C. King, C. J. Pudsey, and J. Turner (2003), Recent rapid regional climate warming on the Antarctic Peninsula, *Clim. Change*, *60*, 243–274.

Watkins, A. B., and I. Simmonds (1999), A late spring surge in the open water of the Antarctic sea ice pack, *Geophys. Res. Lett.*, *26*(10), 1481–1484.

Watkins, A. B., and I. Simmonds (2000), Current trends in Antarctic sea ice: The 1990s impact on a short climatology, *J. Clim.*, *13*, 4441–4451.

Yuan, X. (2004a), ENSO-related impacts on Antarctic sea ice: A synthesis of phenomenon and mechanisms, *Antarct. Sci.*, *16*(4), 415–425.

Yuan, X. (2004b), High wind evaluation in the Southern Ocean, *J. Geophys. Res.*, *109*, D13101, doi:10.1029/2003JD004179.

Yuan, X., and D. G. Martinson (2000), Antarctic sea ice extent variability and its global connectivity, *J. Clim.*, *13*, 1697–1717.

Yuan, X., and D. G. Martinson (2001), The Antarctic Dipole and its predictability, *Geophys. Res. Lett.*, *28*(18), 3609–3612.

Zwally, J. H., J. C. Comiso, C. L. Parkinson, D. J. Cavalieri, and P. Gloersen (2002), Variability of Antarctic sea ice 1979–1998, *J. Geophys. Res.*, *107*(C5), 3041, doi:10.1029/2000JC000733.

D. G. Martinson, S. E. Stammerjohn, and X. Yuan, Lamont Doherty Earth Observatory, Columbia University, Palisades, NY 10964, USA. (sstammerjohn@giss.nasa.gov)

D. Rind, NASA Goddard Institute for Space Studies, 2880 Broadway, New York, NY 10025, USA.

R. C. Smith, Institute for Computational Earth System Science, University of California, Santa Barbara, CA 93106, USA.